

Topical Editor Decision: Reconsider after major revisions (further review by editor and referees) (26 Mar 2019) by Andrew J. Kavanagh

Comments to the Author:

Thank you for taking part in the interactive discussions. In the next step of the review process I would like to ask the reviewers to have another look at the manuscript to assess whether you have addressed their concerns. To do this, can I request that you upload your response to the reviewers as detailed in this email.

Dear Editor: Really thank you very much for your kindly comments and decision. Detailed responses to the reviewers are given as follows. The revised manuscript with tracked changes is also attached later.

Response to the reviewer #1

Interactive comment on “High-resolution Beijing MST radar detection of tropopause structure and variability over Xianghe (39.75° N, 116.96° E), China” by Feilong Chen et al.

Anonymous Referee #1

Received and published: 21 February 2019

Summary

Chen and co-authors use a VHF wind-profiling radar to examine the structure and variability of the tropopause over Xianghe, China with high temporal resolution. The authors use the gradient of the return power to identify the radar tropopause (RT) and compare with lapse-rate tropopauses (LRT) calculated from radiosondes which are launched some 45km away. The RT and LRT agree fairly well: the authors speculate that the non-perfect correlations are due to the seasonal movement of the sub-tropical jet. Chen and co-authors also investigate the tropopause sharpness and the relation between RT and the 2PVU dynamical tropopause and briefly mention the synoptic meteorology likely contributing to the similarities and differences between these tropopause definitions.

As Chen and co-authors cite in their manuscript, there have been several papers discussing the structure of the RT at varying latitudes in recent years. It seems that there is a bit of a renaissance in papers on this subject following the early study of Gage & Green (1979). The ability of VHF radars to sample sub-diurnal tropopause structure still must be of interest to the community.

Furthermore, the latitude of Xianghe at 40N is interesting for sub-diurnal and synoptic-scale tropopause variability given the seasonal movement of the sub-tropical jet of-ten creating two tropopauses which allows for significant stratosphere-troposphere ex-change. Unfortunately, Chen and colleagues choose to reject any analysis of the second, higher, tropopause in this paper which would have added significant interest to their analysis. As such, as it stands, this paper contains little new or interesting science.

I would therefore like the authors to implement the following recommendations in order to increase the scientific value and interest of their study.

Paper references are given at the end.

Response:

Dear reviewer, We really thank you for the helpful and constructive comments, which will be of great useful for this article. We hope that the reviewers will be satisfied with our responses and revisions. Our responses are in different color style (reviewer's comments are shown in black and our response in blue type).

Response regarding to the comment: 'The RT and LRT agree fairly well: the authors speculate that the non-perfect correlations are due to the seasonal movement of the sub-tropical jet'. Statistically, our results found that the agreement between the RT and LRT height is similarly well during different seasons. We speculate that the relatively poor agreement between the RT/LRT and PVT in summer and late autumn is probably due to the seasonal movement of the sub-tropical jet.

Regarding the second tropopause, detailed responses are given below.

Regarding the scientific value:

Firstly, this paper used the latest data set of Beijing MST radar (more than 5 years since the routine operation of the radar) to study the high-resolution tropopause structure over Xianghe and then compared it with LRT and PVT. The results of this paper are of great guiding significance to readers who want to make use of the Beijing MST data to study various interesting topics (especially the tropopause variation).

Secondly, there are few statistical studies on the tropopause structure at near 40N with high temporal resolution. By comparing with LRT, we verified the potential of Beijing MST radar to identify tropopause. Diurnal variations of the tropopause with high temporal resolution are also analyzed. The echo power intensity, wind field intensity and wind data acquisition rate near the tropopause are also analyzed.

Major Comments

1) Line 101. You write that you will focus on the first (lowest) tropopause here. Yet I would argue that by neglecting the second tropopause, you are majorly limiting the value of your science. For example, by also characterising the second tropopause, you would likely answer some of your speculations regarding the differences between RT, LRT which you make in the Conclusions. Examining the seasonal variations of both tropopauses with radar would be a useful contribution to the literature and should be done in this paper.

Response:

Dear reviewer, the identification and observation of the second tropopause (characterized by tropical features and located near 16 km) is not considered by both the RT definition and LRT definition. The second tropopause (if it existed) can be well detected by radiosonde soundings. However, the low mode observations of Beijing MST radar have a limited highest detectible altitude of ~13-14 km (in vertical direction), thus the routine second tropopause is impossible to be detected under low mode

observation. The middle mode observations of Beijing MST radar can reach as high as 24 km, but its altitude resolution is relatively poor with value of 600 m, while the resolution in low mode is 150 m. Thus, the middle mode data is not appropriate to be used to detect high resolution tropopause structure, otherwise will lead to a large error by the limited altitude resolution.

Given that we focused on the first tropopause structure using both the RT and LRT definitions, some responses are needed regarding the differences between RT and LRT. The second tropopause structure may hardly an important factor causing the differences between RT and LRT. As mentioned in the manuscript (discussion section) that some specific meteorological processes can lead to the ambiguities and indefiniteness in thermal and radar definitions, such as fronts, cyclones or typhoons, and folding. Such ambiguities often result in large difference in altitude between the RT and LRT. In addition, when multiple temperature inversion layers (sometimes can be called as multiple tropopauses, sometimes can not, depending on if the inversion layers meet the WMO LRT definition) occurred below 16 km, the RT generally matched the lower part and LRT often matched the upper part, such as the double layers of enhanced echo power shown in Figure 3 on 4 and 5 February 2012.

2) Line 230 regarding the low correlations during summer and autumn. Although the RT and PV tropopauses are both dynamical tropopause definitions, we would not always expect close agreement especially during the passage of cyclones. Still, these larger offsets during summer (Fig 6c) are interesting. Does this suggest that the 2PVU sur-face is not the best measure of a dynamical tropopause above Beijing during summer-time? Given that you only consider 'low-mode' tropopauses, maybe you are missing most of the summer high tropopauses (see Major Point 3 below) which may account for some differences? You should separate the tropopause data into cyclonic / anti-cyclonic conditions, as you should then discover the reasons for the difference – my expectations is that you should see closer agreement between the definitions during anti-cyclonic conditions than during cyclonic. Also, you should separate the data into single tropopause / double tropopause times to investigate the RT – PV tropopause relationships more fully.

Response:

Yes, these larger offsets during summer (Fig 6c) are probable suggest that the 2PVU sur-face is not the best measure of a dynamical tropopause above Beijing during summer-time. We consider that these differences are less related to the missing of summer high tropopause (second tropopause near ~16 km).

Firstly, during autumn and summer, most of the comparison data pairs located in the left-side of 1:1 line (Fig. 6c and 6d), indicating most of the RT are located higher than the 2PVU tropopause height.

Secondly, if the differences are closely associated to the missing of second tropopauses, the distribution of the scatter points in Figure 6c should be that: most of the comparison data pairs located in the right-side of 1:1 line.

Based on the comments and response above, we have added the following sentences in the revised manuscript (discussion section):

‘The existing cyclones or anticyclones in the upper-troposphere (Wirth, 2000), of course, may also be an important cause of the significant asymmetric differences (most of the scattered points deviate significantly from the 1:1 line). This asymmetric differences, that is most of the RT are located higher than the 2PVU tropopause height, suggest that the 2PVU surface is not the best measure of a dynamical tropopause over Beijing during summer-time.’.

Certainly, cyclonic and anti-cyclonic conditions may also be an important influence factor for the differences between RT and PVT (Wirth, 2001). More detailed discussion about the striking asymmetric differences in height between LRT/RT and PVT will not be given in this paper.

Wirth, V.: Thermal versus dynamical tropopause in upper-tropospheric balanced flow anomalies. Quarterly Journal of the Royal Meteorological Society, 126(562), 299-317, 2000.

3) Discussion section and Figure 12a. I am surprised that you can't detect the thermal (lapse-rate) tropopause in the radiosonde profile at 16km. In such cases, as your radar 'low mode' doesn't reach high enough, you should switch to analysing 'mid-mode' to find the radar tropopause. On line 300 you say that the 16km inversion is the 'sec-ond tropopause' but clearly it's the first tropopause, because it is the lowest altitude tropopause. Presumably on this day, you are observing a tropical-like atmosphere with a very high tropopause. You should be aware that at a similar latitude to the Beijing radar is the MU radar in Shigaraki, Japan (35N), where high-time resolution radiosonde and radar analyses over many decades have demonstrated the very high summer-time radar and radiosonde tropopauses (first tropopause) at altitudes above 15km (please refer to Tsuda et al., 1991; Hermawan et al., EPS, 1998; Alexander & Tsuda, JTech, 2008, for further details). You need to include analysis of your higher-altitude tropopause in your study, regardless of whether it's the first or second tropopause.

Response:

We thought about this a lot during this statistical study.

The inversion layer near 16 km or higher is indeed meet the LRT definition. However, considering that the radar station is located at the middle latitude of 40N and the mechanism of formation of the second tropopause (Pan et al., 2004; Randel et al., 2007; Pan et al., 2009), the inversion height at a height of ~16km (or higher) over the radar station is the second tropopause with tropical characteristics. In fact, the routine occurred second tropopause is almost located near 16km altitude throughout the seasons. In a word, no matter whether the inversion layer at ~16 km is the first tropopause or the second tropopause, such tropical featured higher tropopause will not be considered and studied here.

Therefore, we explain in the introduction that this study only focuses on the first tropopause below 16km, no matter whether it exists or not. Indeed, the routine presented higher tropopause (second tropopause near 16km) in different seasons throughout the year is worthwhile for studying. In view of the limitation of the altitude

resolution of the middle mode data in the Beijing MST radar (with value of 600m), it was not used to study the tropical featured second tropopause near 16km, especially for the statistical study. The case observation of the second tropopause near 16km using the middle mode is worthy of future study.

In order to avoid misguidance and to fit in with the main research focus of this paper, we have indicated in many places that the research focus of this paper is the first tropopause under 16km (as long as it exists).

For example, one sentence has been modified in the introduction section of the revised manuscript: ‘In the present study, we focus only on the first tropopause (below 16 km) which will be referred to as ‘tropopause’ hereafter’.

In addition, the figure 12 and the figure caption have also been modified accordingly:

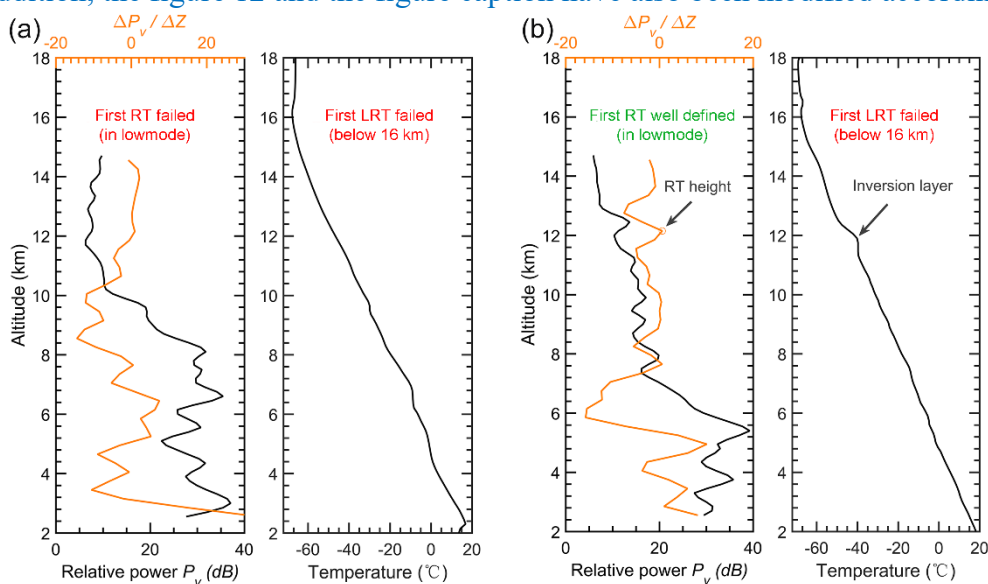


Figure 12. Example profiles of radar echo power and radiosonde temperature that (a) both the RT and LRT definitions fail due to the continuing decrease in temperature on 00 UTC 7 July 2012 and (b) the temperature inversion layer failed to meet the LRT definition but well defined in RT definition on 12 UTC 02 August 2012. Please note that we only consider the conditions below 16 km.

Pan, L. L., Randel, W. J., Gary, B. L., Mahoney, M. J., and Hints, E. J.: Definitions and sharpness of the extratropical tropopause: A trace gas perspective. *Journal of Geophysical Research*, 109, D23103, doi:10.1029/2004JD004982, 2004.

Pan, L. L., W. J. Randel, J. C. Gille, W. D. Hall, B. Nardi, S. Massie, V. Yudin, R. Khosravi, P. Konopka, and D. Tarasick: Tropospheric intrusions associated with the secondary tropopause, *Journal of Geophysical Research*, 114, D10302, 2009.

Randel, W. J., Seidel, D. J., and Pan, L. L.: Observational characteristics of double tropopauses. *Journal of Geophysical Research*, 112, D07309, 2007.

Minor Comments

1) Line 51: ‘Radiosonde sounding. . . impractical [spelling!] in severe weather’. This isn’t really

true. The sentence suggests to the reader that radiosondes cannot be launched in heavy rainfall yet they are in the tropics, nor in the cold, yet they are in the polar regions. I suggest removing this sentence.

Response:

Really thanks for pointing out the flaw. The corresponding sentence has been removed.

2) Line 62. So the best way forward is to create a 'blended tropopause' for the globe as Wilcox et al. (QJRMS 2011) did. I suggest you read and cite this paper here.

Response:

Really thanks for recommending this valuable paper. This paper has been cited in the revised manuscript. Following sentence has been added in the revised manuscript: 'Creating a 'blended tropopause' for the globe may probable a good way forward (Wilcox et al., 2011).'

3) Line 63. Before discussing VHF radars, you should briefly discuss the use of GPS radio occultation satellites which provide highly accurate, climatically stable measure-ments of temperature and thus of the tropopause. There are many papers on this subject which you can easily find. Some valuable ones include: Schmidt et al., ACP 2005; Son et al., JGR 2011.

Response:

Yes, it is necessary to briefly discuss the use of GPS radio occultation satellites to study the tropopause. The corresponding references have been cited in the revised manuscript. Following sentence is added in the revised manuscript: 'In addition, the data of GPS radio occultation satellites is also an effective way and commonly applied to study tropopause (e.g. Schmidt et al., 2005; Son et al., 2011).'

4) Line 71. I cannot find the paper Alexander et al (2012). I think you are accidently quoting the ACPD submitted manuscript paper rather than the final ACP paper. You should cite the final, ACP paper as: Alexander et al. (2013). See the 'References' section below for the proper reference.

Response:

Really thanks for pointing out the flaw. It has been corrected in the revised manuscript.

5) Line 102. For what purpose is the high temporal resolution 'still insufficient'? Why do we care about obtaining the tropopause at hourly time-scales?

Response:

Yes, the expression of this sentence is inaccurate. We have deleted the sentence in the revised manuscript.

6) Line 209, sentence: 'Fig 4 explicitly indicates the good capability of the Beijing MST radar. . .' No it doesn't. Figure 4 shows that the radar tropopause determined by this radar shows reasonable agreement with radiosonde-derived lapse rate tropopauses and that the differences are mostly under 1km.

Response:

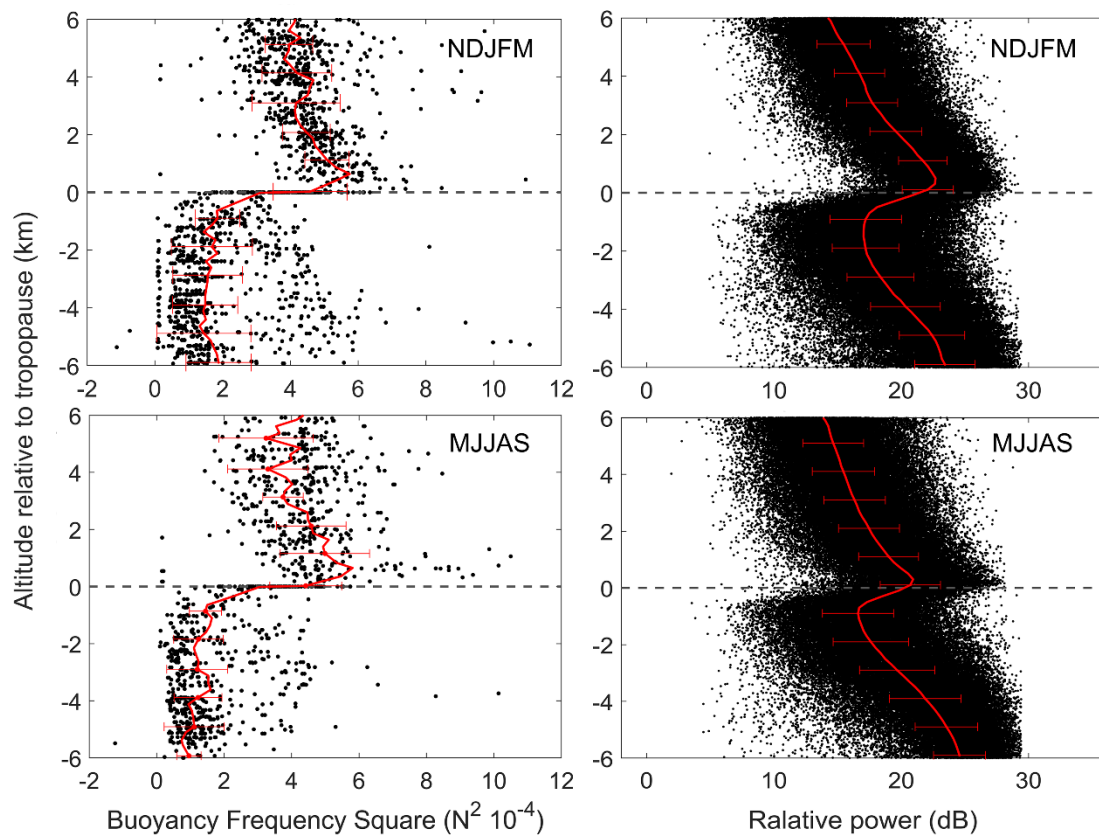
Yes, the expression of this sentence is inaccurate. The corresponding sentence has been

changed to ‘Fig. 4 explicitly shows that the RT derived by the Beijing MST radar agrees reasonably well with the LRT throughout the seasons.’ in the revised manuscript.

7) Line 245: I can’t see these differences clearly in Figure 7. On top of your dot points in Figure 7, please plot the mean and standard deviations at each altitude. Please describe in the text what new information this plot shows – after all, the community well knows about the sudden jump in N^2 at the tropopause and the jump in radar power too.

Response:

Yes, you are right. It is necessary to plot the mean and standard deviations in each panel of Figure 7. Really thanks for your comments. The mean values and error bars are plotted in Figure 7 in the revised manuscript.



Indeed, the sudden jump in both the static stability and radar echo power upon the tropopause is commonly well known. Several other features seen from the figure have been reported in the revised manuscript: ‘The degree of sudden increase in echo power is more gradual than that in static stability. The amplitude of the sudden increase in radar power experienced a slightly larger during NDJFM than that during MJJAS (red lines of right panels). Another interesting feature in the lower-stratosphere is that both the static stability and radar power points show less disperse during NDJFM than that during MJJAS.’.

8) Line 312 onwards (comments about Figure 12b and the inversion at 12km). A simple way around this is to set some threshold in your radar tropopause algorithm to avoid these small peaks. And again, you should switch to ‘mid-mode’ analysis here.

Response:

Because the radar echo power is associated with various situations. Threshold may not be appropriate for Beijing MST radar. Furthermore, the phenomenal of enhanced gradient in radar echo power is real, and it just correspond well to the relatively weak inversion of radiosonde temperature near 12 km.

9) Line 326 and comments about cyclones / anti-cyclones. This is easy to investigate and should be done rather than just speculating. See my Major Comments above.

Response:

Dear reviewer, really thanks for your comments. Certainly, cyclonic and anti-cyclonic conditions are interesting topics. But it will not be studied in detail in this paper and this is beyond the scope of this article.

Technical:

1) Line 250: Avoid using the word 'inversion' unless referring to the increase in temperature with altitude

Response:

Yes, you are right. The corresponding sentence has been modified to 'Clearly, both profiles exhibit a sudden increase with height near the tropopause' in the revised manuscript.

2) Figure 3. I can't see the green asterisks. Please choose a different colour to make this clear

Response:

Really thanks for pointing out the flaw. Fig.3 has been corrected in the revised manuscript.

3) Figure 7. The means (and standard deviations) should be overplotted

Response:

Really thanks for pointing out the flaw. The means and standard deviations are plotted in each panel of Figure 7.

4) Figure 8. Please clarify the x-axis 'Data acquisition rate'. Is this the percentage of (useful) signal returned, or is it the percentage of wind data collected or what?

Response:

Really thanks for your comments. Data acquisition rate indicates the effective wind data. It has been corrected in the 3.3 section and the figure caption in the revised paper.

5) Figure 12, as discussed in the Minor Comments above, you should be switching to 'mid-mode' to identify the high-altitude tropopause, which in these instances is still the 'first tropopause'

Response:

As mentioned above and explained in many parts of the article, we only focus on the tropopause below 16km. The tropopause near 16 km or above is not subject to

consideration (statistical analysis). For example, one sentence in the introduction section of the revised manuscript: ‘In the present study, we focus only on the first tropopause (below 16 km) which will be referred to as ‘tropopause’ hereafter’.

References:

Alexander, S.P., Murphy, D.J., and Klekociuk, A.R., 2013, High resolution VHF radar measurements of tropopause structure and variability at Davis, Antarctica (69° S, 78° E), *Atmos. Chem. Phys.*, 13, 3121-3132, doi:10.5194/acp-13-3121-2013

Alexander, S. P. and Tsuda T., 2008, ‘High Resolution Radio Acoustic Sounding System (RASS) Observations and Analysis up to 20km’, *Journal of Atmospheric and Oceanic Technology*, 25, 8, p1383-1396, doi: 10.1175/2007JTECHA983.1

Hermawan, E., and T. Tsuda, 1999: Estimation of turbulence energy dissipation rate and vertical eddy diffusivity with the MU radar RASS. *J. Atmos. Solar-Terr. Phys.*, 61, 1123–1130.

Schmidt, T., Heise, S., Wickert, J., Beyerle, G., Reigber, C., 2005, GPS radio occultation with CHAMP and SAC-C: Global monitoring of thermal tropopause parameters, *Atmos. Chem. Phys.*, 5, 1473–1488

Son, S.-W., Tandon, N.F., Polvani, L.M, 2011, The fine-scale structure of the global tropopause derived from COSMIC GPS radio occultation measurements, *J. Geophys. Res.*, 116, D20113, doi: 10.1029/2011JD016030

Tsuda, T., T. E. VanZandt, M. Mizumoto, S. Kato, and S. Fukao, Spectral analysis of temperature and Brunt Väisälä frequency fluctuations observed by radiosondes, *J. Geophys. Res.*, 96, 17265–17278, 1991.

Wilcox L.J., Hoskins B.J., Shine K.P. 2012. A global blended tropopause based on ERA data. Part I: Climatology. *Q. J. R. Meteorol. Soc.* 138: 561–575. DOI:10.1002/qj.951.

Really thanks for recommending these valuable references.

Thank you again for your help with improving the paper.

Best regards

Response to the reviewer #2

Interactive comment on "High-resolution Beijing MST radar detection of tropopause structure and variability over Xianghe (39.75° N, 116.96° E), China" by Feilong Chen et al.

Anonymous Referee #2

Received and published: 18 March 2019

In this study, the authors demonstrated the potential of MST radar in detecting the tropopause height (RT) from the radar backscattered echo power profiles by carrying out extensive comparison with the lapse rate tropopause (LRT) derived from radiosonde data and with dynamical tropopause (2 PVU) derived from ERA-Interim re-analysis dataset during the period Nov. 2011 to May 2017 covering all seasons. Comparison results showed good agreement between Radar and radiosonde and that between radar and ERA data in most of the seasons. The RT determination and comparison with other observations has been already carried out by many other investigators. However, a systematic comparison has been carried out in this paper and the difference in tropopause height is attributed to the sharpness of the tropopause inversion layer (weak / strong). The potential of radar in examining the short-term variability of tropopause useful for wave studies etc and its limitation in detecting tropopause in few occasions are also discussed. In general, the paper is well written and the results are interesting. However, a few concerns need to be addressed, before the manuscript is published.

Response:

Dear reviewer, we really thank you for the helpful and constructive comments, which will be of great useful for this article. We hope that the reviewers will be satisfied with our responses and revisions. Our responses are in different color style (reviewer's comments are shown in black and our response in blue type).

1) RT is determined using the vertical beam echo power data collected in "low mode" operation (which receives strong signal up to 14-15 km). In "middle mode", strong signals can be obtained in the altitude region 7-25 km (as seen in Fig.8). Also, the "first tropopause" and "second tropopause" (based on WMO definition of LRT) are clearly evident in the mean effective data acquisition data obtained from middle mode operation (Fig.8). I strongly believe, that if "middle mode" vertical beam data is used, the strong gradients in radar echo power could be discernible corresponding to the altitudes of first and second tropopause. The authors can examine this aspect for available dataset in middle mode observations and compare with the first and second tropopause derived from radiosonde data.

Response:

Yes, you are right. Really thanks for your valuable comments. It is necessary to explain here the concerns about the radar tropopause detection using middle mode data.

Firstly, the middle mode data is not appropriate to be used to detect the clear tropopause structure (both the first or the second tropopause). Figure R1 (shown below) shows the middle mode observation results of the altitude-time intensity plot of radar backscattered echo power on February 2014. The month is the same as that in Figure 3 of the manuscript. Indeed, the first tropopause structure can be seen with middle mode observations, but the boundary is unsharpness and too coarse to identify the clear tropopause height, at least (especially) compared to the Figure 3 in the manuscript. In addition, also is the most important feature, the second tropopause is barely detected by middle mode results. The limited altitude resolution (600 m) and the limited radar transmitted power are likely the main causes.

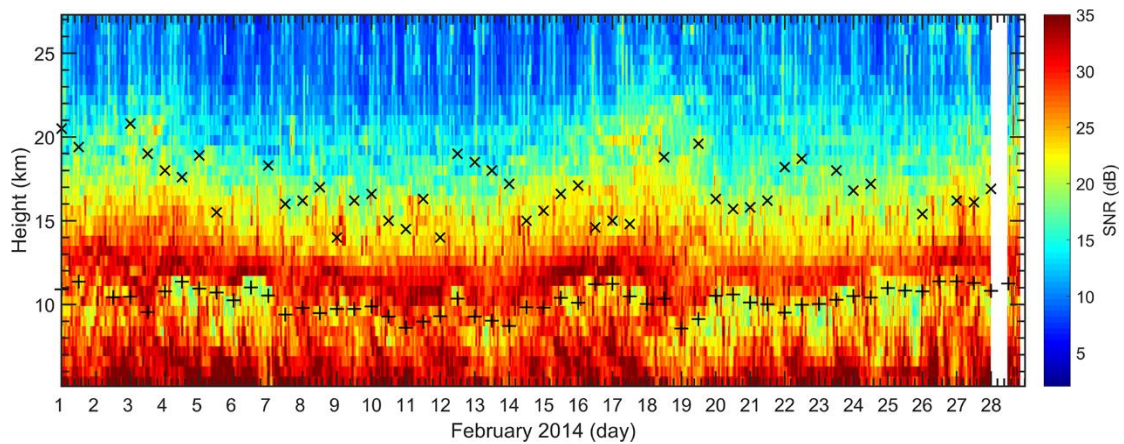


Figure R1. Middle mode observation results: Altitude-time intensity plot of radar backscattered echo power for February 2014. ‘+’ indicates the first tropopause; and ‘x’ denotes the higher second tropopause derived from radiosonde data.

Secondly, why the “first tropopause” and “second tropopause” appeared to be clear in the mean effective data acquisition rate (profile) obtained from middle mode operation (Fig.8)? We believe that this is largely because the data acquisition rate is the statistical result of five-year dataset, even if the height resolution is relatively low (600 m), the 5-year statistics are enough to amplify the impact of changes in atmospheric states (such as the static stability) around the transition region (between the troposphere and the stratosphere) on the data acquisition rate.

Finally, some responses regarding to the second tropopause:

Considering that the mechanism of the formation of second tropopause (Pan et al., 2004; Randel et al., 2007; Pan et al., 2009), the inversion height of ~16km (or higher) over the radar station is the second tropopause with tropical characteristics. Anyhow, no matter whether the inversion layer at ~16 km is the first tropopause or the second tropopause, such tropical featured higher tropopause will not be considered and studied

here by both the RT definition and LRT definition. Indeed, the routine presented higher tropopause (second tropopause near 16km) in different seasons throughout the year is worthwhile for studying. However, due the relatively poor altitude resolution for middle mode data, it is not appropriate to be used to detect high resolution tropopause structure over Beijing MST radar station, especially for the statistical study. The case observation of the second tropopause near 16 km (or higher) using the middle mode data is worthy of future study.

Therefore, we explain in many places that this study only focuses on the first tropopause below 16km, no matter whether it exists or not. For example, one sentence has been modified in the introduction section of the revised manuscript: ‘In the present study, we focus only on the first tropopause (below 16 km) which will be referred to as ‘tropopause’ hereafter’.

Pan, L. L., Randel, W. J., Gary, B. L., Mahoney, M. J., and Hints, E. J.: Definitions and sharpness of the extratropical tropopause: A trace gas perspective. Journal of Geophysical Research, 109, D23103, doi:10.1029/2004JD004982, 2004.

Pan, L. L., W. J. Randel, J. C. Gille, W. D. Hall, B. Nardi, S. Massie, V. Yudin, R. Khosravi, P. Konopka, and D. Tarasick: Tropospheric intrusions associated with the secondary tropopause, Journal of Geophysical Research, 114, D10302, 2009.

Randel, W. J., Seidel, D. J., and Pan, L. L.: Observational characteristics of double tropopauses. Journal of Geophysical Research, 112, D07309, 2007.

2) Radar provides a vertical resolution of 150 m in "low mode" and 600 m in "middle mode" and "1200 m" in "high mode" and the temporal resolution is about 30 minutes. In the present study, RT derived from the vertical beam data in low mode is compared with the dynamical tropopause (2PVU) derived from potential vorticity obtained from ERA-interim reanalysis. The comparison results shows large deviation between the two. Fine resolution radar data is compared with the coarse resolution ERA dataset. What is sanctity in comparing these two datasets.

Response:

Dear reviewer, really thanks for your comments. The difference in height resolution between radar and reanalysis data is unlikely to be one reason for the large difference between RT and PVT. There are also differences in resolution between radar and radiosonde data. At least, the difference in height resolution is not the main point. The interesting features from the comparison results between RT and PVT are that: the RTs agree reasonably well with the PVTs with the correlation coefficient of 0.72 and 0.76 respectively, during winter and spring (Fig. 6a and 6b). In contrast, the consistency for summer (Fig. 6c) is relatively bad and with correlation coefficient of only 0.33.

Whereas, in contrast, previous research about the RT and PVT results over polar regions

by Alexander et al., (2013) reported that the comparison between the RT and PVT showed the similar good agreement during both summer and winter.

The possible causes of the larger offsets during summer (Fig 6c) is discussed in the revised manuscript. Following sentences in the revised manuscript (discussion section) have been added: ‘The existing cyclones or anticyclones in the upper-troposphere (Wirth, 2000), of course, may also be an important cause of the significant asymmetric differences (most of the scattered points deviate significantly from the 1:1 line). This asymmetric differences, that is most of the RT are located higher than the 2PVU tropopause height, suggest that the 2PVU surface is not the best measure of a dynamical tropopause over Beijing during summer-time.’.

Alexander, S.P., Murphy, D.J., and Klekociuk, A.R.: High resolution VHF radar measurements of tropopause structure and variability at Davis, Antarctica (69° S, 78° E), Atmos. Chem. Phys., 13, 3121-3132, 2013.

Specific/Minor comments

Line 28 : replace "good capability of Beijing MST radar" with "potential of Beijing MST radar "

Response:

Really thanks for pointing out the flaw. The corresponding sentence has been replaced.

Lines 108, 246, Fig. 8: Is this the "data acquisition rate" of backscattered echo power received?. Effective data acquisition rate for different modes of radar operation are shown? How is this parameter estimated. Give details.

Response:

Really thanks for your comments. Data acquisition rate indicates the effective wind data. It has been corrected in the 3.3 section and the figure caption in the revised paper.

Lines 165-168: The method of identifying dynamical tropopause from potential vorticity is to be added. ERA-interim reanalysis data does not have fine vertical resolution. But the dynamical tropopause determined from the above is compared with RT derived from higher vertical resolution radar backscattered echo power. Hence, the larger difference in tropopause height is expected between the two methods.

Response:

Dear reviewer, the difference in height resolution between radar and reanalysis data is unlikely to be one key reason for the large difference between RT and PVT. There are also differences in resolution between radar and radiosonde data. At least, the difference in height resolution is not the main point. The possible causes of the larger offsets during summer (Fig 6c) is discussed in the revised manuscript:

‘The existing cyclones or anticyclones in the upper-troposphere (Wirth, 2000), of

course, may also be an important cause of the significant asymmetric differences (most of the scattered points deviate significantly from the 1:1 line). This asymmetric differences, that is most of the RT are located higher than the 2PVU tropopause height, suggest that the 2PVU surface is not the best measure of a dynamical tropopause over Beijing during summer-time.?

Line 181: delete "fine-scale"

Response:

Really thanks for pointing out the flaw. It has been corrected in the revised manuscript.

Line 190-191: ".....the RT is well defined as the first layer with enhanced echo power..."

Response:

It has been corrected in the revised manuscript.

Line 209: replace "good capability" with "potential"

Response:

It has been corrected in the revised manuscript.

Line 217: "sharpness of tropopause" is affected by cyclonic /anticyclonic systems. Explain. Are radar measurements carried out during such systems. please clarify.

Response:

Dear reviewer, we didn't demonstrat that the sharpness of tropopause is affected by cyclonic /anticyclonic systems. The results form Figure 5 indicate that the larger (weaker) tropopause sharpness contribute to lower (higher) difference between the RT and LRT.

Line 237, 246: what is "effective data acquisition rate?: Middle mode observation in Figure 8 shows two distinct peaks corresponding to the mean of first and second tropopauses based on LRT definition by WMO. Then why the data obtained from this mode (middle mode) is not used for the extensive comparison of first and second tropopause derived from radiosonde dataset, which is not so far studied extensively.

Response:

Really thanks for your comments. Data acquisition rate indicates the effective wind data. It has been corrected in the 3.3 section and the figure caption in the revised paper. Firstly, no matter whether the inversion layer at ~16 km is the first tropopause or the second tropopause, such tropical featured higher tropopause will not be considered and studied here by both the RT definition and LRT definition. Secondly, the middle mode data is not appropriate to be used to detect the clear tropopause structure (both the first or the second tropopause, please see Figure R1 above). Detailed responses about the issue of second tropopause are given above.

Lines 247-249: Correct this sentence (message not clear).

Response:

Really thanks for your comments. It has been corrected in the revised manuscript.

Line 272: "...radar-derived winds are combined...." what does it mean?

Response:

Really thanks for pointing out the flaw. The corresponding sentence has been corrected in the revised manuscript and modified to 'With the absence of temperature measurements, zonal and meridional winds are applied to demonstrate the evidence of diurnal or semidiurnal modulation by tidal'.

Line 289-290: correct the sentence

Response:

Really thanks for pointing out the flaw. The corresponding sentence has been corrected in the revised manuscript.

Line 293-294: what are the system problems that makes RT identification difficult?

Response:

The corresponding sentence has been changed to 'Apart from the system problems (e.g. the damage of T/R module)' in the revised manuscript.

Lines: 297-298: correct the sentence

Response:

It has been corrected in the revised manuscript.

Line 300: In this case, the temperature inversion is observed at 16 km...

Response:

Detailed responses about the issue of second tropopause are given above. In order to avoid the potential misguidance and to fit in with the main research focus of this paper, we have indicated in many places that the research focus of this paper is the first tropopause below 16km (as long as it exists).

For example, one sentence has been modified in the introduction section of the revised manuscript: 'In the present study, we focus only on the first tropopause (below 16 km) which will be referred to as 'tropopause' hereafter'.

In addition, the figure 12 and the figure caption have also been modified accordingly:

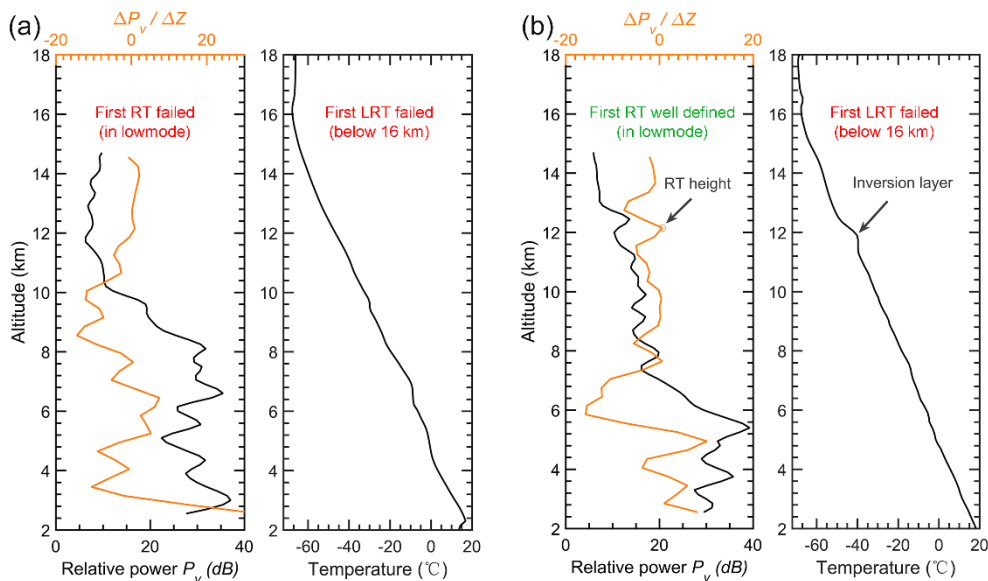


Figure 12. Example profiles of radar echo power and radiosonde temperature that (a) both the RT and LRT definitions fail due to the continuing decrease in temperature on 00 UTC 7 July 2012 and (b) the temperature inversion layer failed to meet the LRT definition but well defined in RT definition on 12 UTC 02 August 2012. Please note that we only consider the conditions below 16 km.

Line 307-308: Correct this sentence....

Response:

Really thanks for pointing out the flaw. The corresponding sentence has been corrected

Line 311: ..difficult in identifying the thermal tropopause from radiosonde profiles ..

Response:

Really thanks for your comments. It has been corrected in the revised manuscript.

Line 313: ...altitude extent of inversion layer is too thin to meet the WMO criterion...

Response:

Really thanks. It has been corrected in the revised manuscript.

Line 316: delete "Need to highlight again that"

Response:

Really thanks. It has been deleted in the revised manuscript.

Line 324: inconsistency between the RT and PVT

Response:

Really thanks. It has been corrected in the revised manuscript.

Line 326-327: Confirm whether radar measurements are carried out during cyclones/anticyclones in the upper troposphere (which period/season). Is the asymmetric differences in tropopause heights mainly due to the above conditions or due to difference in vertical resolution of radar and ERA dataset.

Response:

Dear reviewer, the difference in height resolution between radar and reanalysis data is unlikely to be one key reason for the large difference between RT and PVT. There are also differences in resolution between radar and radiosonde data. At least, the difference in height resolution is not the main point. Because the differences during spring and winter is not so bad as that during summer. The possible causes of the asymmetric differences during summer (Fig 6c) is discussed in the revised manuscript:

‘The existing cyclones or anticyclones in the upper-troposphere (Wirth, 2000), of course, may also be an important cause of the significant asymmetric differences (most of the scattered points deviate significantly from the 1:1 line). This asymmetric differences, that is most of the RT are located higher than the 2PVU tropopause height, suggest that the 2PVU surface is not the best measure of a dynamical tropopause over Beijing during summer-time.’.

Wirth, V.: Thermal versus dynamical tropopause in upper-tropospheric balanced flow anomalies. Quarterly Journal of the Royal Meteorological Society, 126(562), 299-317, 2000.

Thank you again for your help with improving the paper.

Best regards

1 **High-resolution Beijing MST radar detection of tropopause structure and**
2 **variability over Xianghe (39.75° N, 116.96° E), China**

3 Feilong Chen¹, Gang Chen^{1*}, Yufang Tian², Shaodong Zhang¹, Kaiming Huang¹,
4 Chen Wu¹, Weifan Zhang¹

5 ¹School of Electronic Information, Wuhan University, Wuhan 430072, China.

6 ²Key Laboratory of Middle Atmosphere and Global Environment Observation, Institute
7 of Atmospheric Physics, Chinese Academy of Sciences, Beijing 100029, China.

8 *Corresponding author: Gang Chen (g.chen@whu.edu.cn)

9
10 **Abstract.**

11 As a result of partial specular reflection from the atmospheric stable layer, the radar
12 tropopause (RT) can simply and directly be detected by VHF radars with vertical
13 incidence. Here, the Beijing MST radar measurements are used to investigate the
14 structure and the variabilities of the tropopause in Xianghe, China with a temporal
15 resolution of 0.5 hour from November 2011 to May 2017. High-resolution radar-
16 derived tropopause is compared with the thermal lapse-rate tropopause (LRT) that
17 defined by the World Meteorological Organization (WMO) criterion from twice daily
18 radiosonde soundings and with the dynamical potential vorticity tropopause (PVT) that
19 defined as the height of 2 PVU surface. During all the seasons, the RT and the LRT in
20 altitude agree well with each other with a correlation coefficient of ≥ 0.74 . Statistically,
21 weaker (higher) tropopause sharpness seems to contribute to larger (smaller) difference
22 between the RT and the LRT in altitude. The RT agrees well with the PVT in altitude
23 during winter and spring with a correlation coefficient of ≥ 0.72 , while the correlation

24 coefficient in summer is only 0.33. As expected, the monthly mean RT and LRT height
25 both show seasonal variations. Lomb-Scargle periodograms show that the tropopause
26 exhibits obvious diurnal variation throughout the seasons, whereas the semidiurnal
27 oscillations are rare and occasionally observed during summer and later spring. Our
28 study shows the **potential** of the Beijing MST radar to determine the tropopause height,
29 as well as present its diurnal oscillations.

30 **Key words:** VHF radar; MST radar; tropopause; diurnal oscillation.

31

32 **1. Introduction**

33 The tropopause marks a transition zone separating the well-mixed convectively
34 active troposphere from the stably stratified and more quiescent stratosphere. Its
35 structure and variability is characterized by large changes in thermal (e.g., lapse rate),
36 dynamical (e.g., potential vorticity), and chemical properties (e.g., ozone and water
37 vapor) and hence acts as a key role for the stratosphere-troposphere exchange (STE)
38 processes (Hoinka, 1998; Seidel et al., 2001). The height of the tropopause depends
39 significantly on the latitude, with about 17 km near the equator and less than 9-10 km
40 at polar latitudes (Ramakrishnan, 1933). Over subtropical latitudes with the presence of
41 subtropical jet, where the tropopause experiences rapid change or breaking, tropopause
42 folding events are commonly observed (Pan et al., 2004). Climatologically, the altitude
43 of the tropopause represents the seasonal variation of the flux of stratospheric air
44 intruding into the troposphere (Appenzeller et al., 1996). Moreover, the tropopause
45 height trends can be a sensitive indicator of anthropogenic climate change (Sausen and

46 Santer, 2003; Santer et al., 2003a; Añel et al., 2006).

47 A variety of ways are available to determine the extratropical tropopause.
48 Radiosonde sounding is the most commonly used to define the thermal tropopause
49 (hereafter referred to as LRT) based on temperature lapse-rate (WMO, 1957). The
50 thermal definition of tropopause can be applied globally and the tropopause height
51 easily be determined from one individual profile (Santer et al., 2003). Another feasible
52 definition is to use a specific potential vorticity (PV) surface to represent the dynamical
53 tropopause (hereafter referred to as PVT) (Reed, 1955; Hoskins et al., 1985). Dynamical
54 definition has the advantage that the PV is a conserved property (under adiabatic and
55 friction-less conditions) of an air mass (Hoskins et al., 1985; Bethan et al., 1996). Values
56 in the range 1-4 PVU ($1 \text{ PVU} = 10^6 \text{ m}^2 \text{ s}^{-1} \text{ K kg}^{-1}$) are used in previous researches in the
57 Northern Hemisphere (e.g. Baray et al., 2000; Sprenger et al., 2003; Hoerling et al.,
58 1991). The threshold of 2 PVU surface is the most commonly used (Gettelman et al.,
59 2011). Dynamical definition, however, is not applicable near the equator, where the PV
60 tends to be 0 (e.g., Hoerling et al., 1991; Nielsen-Gammon et al., 2001). **Creating a**
61 **blended tropopause globally may probably a good way forward (Wilcox et al., 2011).**
62 **In addition, the data of GPS radio occultation satellites is also an effective way and**
63 **commonly applied to study tropopause (e.g. Schmidt et al., 2005; Son et al., 2011).**

64 As a result of partial specular reflection from stable atmospheric layer, the radar
65 tropopause (RT) can be well represented and identified by atmospheric radars operating
66 at meter wavelength (VHF band) and directing at vertical incidence (Gage and Green,
67 1979). Research activity increased remarkably following the first report on VHF radar

68 detection of tropopause by Gage and Green (1979), for instance, the researches in
69 middle latitudes (e.g. Hermawan et al., 1998), polar regions (e.g. Hall, 2013a), and
70 tropical regions (e.g. Das et al., 2008; Ravindrababu et al., 2014). Several methods have
71 been proposed to determine the tropopause height via radar echo power, including the
72 largest gradient in echo power (Vaughan et al., 1995; Alexander et al., 2013), the
73 maximum echo power (Vaughan et al., 1995; Hall et al., 2009), and the specific value
74 of echo power (Gage and Green, 1982; Yamamoto et al., 2003). The method of the RT
75 height determination used in this paper will be described in detail in next section.

76 The biggest advantage of the VHF radar measurements is the ability of continuous
77 operation unmanned in any weather conditions. Of course, no definition of the
78 tropopause is perfect. VHF radar system can only be limited to a few locations globally.
79 A detailed review of the close relationship between these different tropopause
80 definitions is provided by Alexander et al., (2012).

81 By means of the radiosonde, reanalysis, and satellite data available globally, long-
82 term (annual or longer) variability in tropopause height has received extensive attention
83 (e.g. Randel et al., 2000; Angell and Korshover, 2009; Son et al., 2011; Liu et al., 2014).
84 However, short period (diurnal or semidiurnal) variability of the tropopause is hard to
85 be examined by these measurements. In contrast, benefiting from the much higher
86 temporal resolution, radar definition of the tropopause provides good capability for
87 studying the diurnal and semidiurnal variation in tropopause height. Earlier, Yamamoto
88 et al., (2003) reported the capability of the Equatorial Atmospheric Radar to examine
89 the diurnal variation of tropopause height. Then, the diurnal variability of the tropical

90 tropopause was investigated in detail by Das et al., (2008) using the Indian Gadanki
91 MST radar. Its diurnal variation over a polar latitude station was investigated by Hall
92 (2013b). In the absence of pressure and temperature parameters, the evidence of
93 atmospheric tides can be well represented by winds (e.g. Huang et al., 2015).

94 The tropopause structure in midlatitudes is different from that in other regions.
95 Double tropopauses structure is a ubiquitous feature over mid-latitude regions near
96 40°N (Pan et al., 2004; Randel et al., 2007). Strong evidence has revealed that the
97 poleward intrusion of subtropical tropospheric air that occurred above the subtropical
98 jet have resulted in the double structure (Pan et al., 2009). The higher part (second
99 tropopause near ~16 km) is characterized by tropical features of cold and higher level,
100 whereas the lower part (first tropopause near ~12 km) is characterized by polar features
101 of warm and lower level. In the present study, we focus **only** on the first tropopause
102 **(below 16 km, if it exists)** which will be referred to as ‘tropopause’ hereafter.

103 In this study, using more than 5 years of Beijing MST radar echo power
104 measurements in vertical beam, we mainly focus on the high-resolution characteristics
105 of the tropopause structure and their comparison with the simultaneous radiosonde and
106 dynamical definitions. Another important objective of this study is to examine the
107 diurnal and semidiurnal variability of the tropopause. The observational characteristics
108 of e.g. winds, echo power, and data acquisition rate near the tropopause layer are also
109 presented in the paper.

110

111 **2. Data and Methods**

112 **2.1. Radar Dataset**

113 As an important part of the Chinese Meridian Project, two MST radar systems are
114 designed and constructed to improve the understanding of the extratropical troposphere,
115 lower stratosphere, and mesosphere (Wang, 2010), which are Wuhan and Beijing MST
116 radars. The Beijing MST radar located in Xianghe, Hebei Province, China (39.75° N,
117 116.96° E, 22 m above sea level) was designed and constructed by the Institute of
118 Atmospheric Physics, Chinese Academy of Sciences and started its routine operation
119 since 20 October 2011 (Tian and Lu, 2017). The radar is a high power coherent pulse-
120 Doppler radar operating at 50 MHz with the maximum peak power of 172 kW and the
121 half-power beam width of 3.2° . Five beams are applied: one vertically pointed beam
122 and four 15° off-zenith beams tilted to north, east, south, and west. In order to obtain
123 the high-quality measurements from troposphere, lower stratosphere, and mesosphere
124 simultaneously, the radar is designed to operate routinely in three separate modes: low
125 mode (designed range 2.5~12 km), middle mode (10~25 km), and high mode (60~90
126 km) with vertical resolutions of 150, 600, and 1200 m, respectively. Under the routine
127 operation, the 15-min break is followed by the 15-min operation cycle (5 min for each
128 mode). As a result, the time resolutions of the low, middle, and high mode
129 measurements are all 30 min. More detailed review of the radar system is given by Chen
130 et al. (2016).

131 Here only the low mode echo power measurements are used to determine the RT
132 height. Although the designed detectable range of the low mode is from 2.5~12 km,
133 the vertically pointed beam can receive stronger echoes from a higher level (~14-15 km)

134 as compared with those from off-vertical beams due to the partial specular reflection
135 mechanism. The measurements in middle mode are also applied to calculate the winds
136 or echo power within ~5-6 km of the tropopause. The parameters for the two routine
137 operation modes are listed in Table 1. The monthly total number of the echo power
138 profiles available in vertical beam (low mode) is shown in Fig. 1. The outliers or
139 severely contaminated data that mainly induced by system problems are eliminated.
140 The large data gap in September is due to the annual preventive maintenance.

141 **2.2. Tropopause Definitions**

142 Due to the large gradient in potential temperature, radar return power received at
143 vertical incidence is significantly enhanced upon the transition zone of the tropopause
144 layer. Using this characteristic, the RT height can be determined effectively by the VHF
145 radar. Here, the RT is defined as the altitude (above 500 hPa) where the maximum
146 vertical gradient of echo power is located (Vaughan et al., 1995; Alexander et al.,
147 2013; Ravindrababu et al., 2014; Chen et al., 2018). Considering the occasional and
148 random noise, to which the derived-RT is sensitive, the echo power profiles are
149 smoothed by a 3-point running mean. In order to further reduce the influence of the
150 noise, the RT definition used here need to satisfy an additional criterion: the determined
151 RT height should be continuous with the adjacent RT heights (one on each side),
152 otherwise to search for the second peak gradient (eliminated if the second peak does
153 not meet the additional criterion). The “continuous” here means that the discrepancy
154 between the two successive heights (in time, 0.5-hour interval) should be <0.6 km. A
155 typical example of the RT and LRT is illustrated in Fig. 2. The LRT is identified based

156 on the World Meteorological Organization (WMO) criteria (WMO, 1957). The radar
157 aspect sensitivity is expressed as the ratio between vertical (p_v) and oblique (p_o) beam
158 echo power (here is 15° east beam). The radiosonde soundings are launched twice daily
159 from the Beijing Meteorological Observatory (39.93°N , 116.28°E , station number
160 54511), which is less than 45 km to the radar site. In this case, the LRT and RT
161 consistent well and are at 11.65 km and 11.85 km respectively. As expected, the LRT
162 characterized by a rapid increase in potential temperature gradient also corresponds to
163 the large gradient in radar aspect sensitivity. Note that the height with maximum value
164 in echo power lie at a higher altitude (as compared with the RT height) of ~ 700 m above
165 the LRT. The dynamical tropopauses used in this paper are derived from the European
166 Centre for Medium-Range Weather Forecasts (ECMWF) ERA-Interim Reanalysis (Dee
167 et al., 2011) and defined as the surface of 2 PVU potential vorticity, which is same to
168 that used by Sprenger et al., (2003) and Alexander et al. (2013).

169 **2.3. Tropopause sharpness definition**

170 For the compared data pairs between the RT and LRT, we calculate the
171 corresponding tropopause sharpness that represents the strength of the tropopause
172 inversion layer. As defined by Wirth, (2000), the tropopause sharpness S_{TP} can be
173 calculated as:

$$174 \quad S_{TP} = \frac{T_{TP+\Delta Z} - T_{TP}}{\Delta Z} - \frac{T_{TP} - T_{TP-\Delta Z}}{\Delta Z} \quad (1)$$

175 where TP denotes the tropopause height, $\Delta Z = 1$ km, and T_{TP} indicates the
176 corresponding temperature. This definition is also used in Alexander et al. 2013 and
177 we're using it for a good comparison with our results.

178 **3. Results**

179 **3.1. High-resolution radar tropopause structure**

180 The height-time cross section of radar echo power and aspect sensitivity is shown
181 in Fig. 3 for a typical month (February 2014), along with the RT, PVT and LRT marked
182 in the figure. In general, the RT agreed well with both the LRT and PVT in height, and
183 most of the RT exhibit a slightly higher altitude. However, the differences between the
184 RT and LRT are sometimes large (reach to ~1-2 km) especially when the RT experience
185 rapid change. Regardless of the background synoptic condition, the difference in the
186 definitions themselves is to a large degree the main contributing factor for the large
187 difference between the RT and LRT. For example, a second layer with significant
188 enhanced echo power is observed above the radar-derived RT for the cases on 4 and 5
189 February 2012 (Fig.3a). According to the definitions, the RT is well defined as the first
190 layer with enhanced echo power and the LRT matched the second layer, similar to that
191 observed by Yamamoto et al., (2003) and Fukao et al., (2003). It is of note that the RT
192 well separates the troposphere characterized by low aspect sensitivity from the lower-
193 stratosphere characterized by high aspect sensitivity (Fig.3b).

194 **3.2. Comparisons between different definitions**

195 To further quantify the consistency and difference in altitude between different
196 tropopause definitions, a detailed comparison is carried out in this section. The seasonal
197 scatterplots for RT versus LRT and the histogram distribution of altitude differences
198 between the RT and LRT are illustrated in Fig. 4, during the period November 2011-
199 May 2017. A total of 2411 data pairs are obtained for comparison. Among them, the

200 number of data pairs is 845 for DJF (winter), 721 for MAM (spring), 321 for JJA
201 (summer), and 524 for SON (autumn). Comparisons have shown a good consistency
202 throughout the seasons and most of the RTs exhibit a slightly higher than the LRTs. The
203 correlation coefficient is 0.74, 0.80, 0.82, and 0.78 for DJF, MAM, JJA, and SON,
204 respectively. The mean and standard deviation difference (RT minus LRT) calculated
205 in DJF, MAM, JJA, and SON is (0.14 ± 0.75) , (0.26 ± 0.78) , (0.33 ± 0.56) , and
206 (0.12 ± 0.69) km, respectively. The proportion of the data pairs with differences <500 m
207 is reasonably good during four seasons and is 63%, 61%, 64%, and 67% for DJF, MAM,
208 JJA, and SON, respectively. **Fig. 4 explicitly shows that the RT derived by the Beijing
209 MST radar agrees reasonably well with the LRT throughout the seasons.**

210 To examine the potential role of the sharpness, Fig. 5a and Fig. 5b show the
211 histogram distribution of the tropopause sharpness along with the probability density
212 curve for data pairs with difference (absolute values of RT minus LRT) <0.5 km and >1
213 km respectively. What is apparent is that most data pairs of Fig. 5a are located to the
214 right (higher sharpness values, with the peak of ~ 7.06 K/km) and of Fig. 5b are to the
215 left (lower sharpness values, with the peak of ~ 6.35 K/km). No matter whether this
216 distribution feature is associated with the cyclonic-anticyclonic systems (e.g. Randel et
217 al., 2007; Randel and Wu, 2010), the results more or less demonstrate that the larger
218 (weaker) tropopause sharpness contribute to lower (higher) difference between the RT
219 and LRT. From the perspective of seasonal statistics, the tropopause sharpness over
220 Beijing station shows similar distribution characteristics throughout the seasons (not
221 shown), which is different from that in polar regions where the sharpness is significantly

222 higher during summer than during winter (Zängl and Hoinka, 2001).

223 The seasonal scatterplots and height difference distribution between the RT and
224 PVT are illustrated and quantified in Fig. 6. The total number of comparing data pairs
225 for winter, spring, summer, and autumn is 1422, 1260, 791, and 1145, respectively.
226 During winter and spring (Fig. 6a and 6b), the RTs agree reasonably well with the PVTs
227 with the correlation coefficient of 0.72 and 0.76 and the mean difference (RT minus
228 PVT) of $(0.55 \pm 0.84 \text{ km})$ and $(1 \pm 0.89 \text{ km})$, respectively. In contrast, the consistency
229 for summer and autumn (Fig. 6c and 6d) is relatively bad and with correlation
230 coefficient of 0.33 and 0.47 and mean difference of $(0.80 \pm 1.39 \text{ km})$ and $(0.75 \pm 1.23$
231 $\text{ km})$, respectively. Especially for summer, the proportion of the comparing data pairs
232 with difference $<0.5 \text{ km}$ is only 10.6% (84). In autumn, need to note that most data pairs
233 with poor consistency is sampled during early autumn.

234 **3.3. Observational characteristics in the vicinity of tropopause**

235 Measurements of radar middle mode are used for examining the horizontal wind,
236 return power, and effective **wind** data acquisition rate within 5-6 km of the tropopause
237 (upper troposphere and lower stratosphere). Left panels of Fig. 7 show the vertical
238 scatterplots of the static stability (represented by the buoyancy frequency squared) as a
239 function of height relative to the LRT and the right panels show the radar echo power
240 as a function of height relative to the RT, during two specific years 2012-2013 for
241 extended winter NDJFM and summer MJJAS seasons. **Mean and standard deviations**
242 **are also plotted in each panel of Fig. 7. As expected, results** clearly show sudden jump
243 in static stability and radar power near the tropopause layer. **The degree of sudden**

244 increase in echo power is more gradual than that in static stability. The amplitude of the
245 sudden increase in radar power experienced a slightly larger during NDJFM than that
246 during MJJAS (red lines of right panels). Another interesting feature in the lower-
247 stratosphere is that both the static stability and radar power points show less disperse
248 during NDJFM than that during MJJAS.

249 Fig. 8 shows the profiles of mean radar effective wind data acquisition rate for low
250 and middle modes during November 2011-May 2017. Clearly, both profiles exhibit a
251 sudden increase with height near the tropopause, with the first peak located ~1 km
252 higher above the mean tropopause height. Note that the second inversion in middle
253 mode profile that occurred near 16 km is associated with the second tropopause. As
254 limited by the highest detectable altitude (the data acquisition rate decreased to lower
255 than 20% at ~16 km), the profile in low mode shows little evidence of second inversion.

256 Fig. 9 shows time-height intensity plot of the monthly mean radar-derived
257 horizontal wind (from middle mode) during November 2011-May 2017, together with
258 the monthly mean location of RT and LRT. One pixel grid denotes 1 month×0.6 km.
259 The monthly mean RT and LRT agreed well with each other in height, within 400 m in
260 August and September and even lower in other months of about within 200 m. They
261 both exhibit a clear seasonal variation, with maximum in early autumn of ~11.6 km and
262 minimum in early spring of ~10.3 km. The monthly mean wind jet varies with season,
263 with the thinnest thickness and lowest strength in summer. The mean tropopause height
264 appears to correspond to the lower boundary location of peak wind layer. The error bars
265 of both the RT and LRT help to illustrate that the tropopauses changes by larger

266 amplitude in winter and June than that in other months.

267 **3.4. Periodogram analysis of the radar tropopause**

268 High temporal resolution detection of tropopause by VHF radar have allowed us
269 to investigate the diurnal or semidiurnal variability of the tropopause. Atmospheric tides
270 are well known global oscillations contributing to the diurnal variation in temperature
271 and background winds, which in turn modulate the tropopause height. With the absence
272 of temperature measurements, **zonal and meridional winds are applied to demonstrate**
273 **the evidence of diurnal or semidiurnal modulation by tidal.** The frequency power
274 spectrum of the RT height, zonal and meridional wind, calculated by means of Lomb-
275 Scargle method (Press and Rybicki, 1989), is illustrated in Fig. 10 for two typical
276 months: May 2015 and December 2016. The choice of Lomb-Scargle algorithm is due
277 to the presence of data gaps (~2 days per week, especially during 2012-2013). The
278 dominant ~24 h periodicity in RT height, zonal and meridional wind is obvious for both
279 months. The evidence of ~12 h period in all three parameters is distinct for May 2015
280 (Fig. 10a), although the power is relatively weaker. Through the analysis for each
281 individual month, we found that the semidiurnal component in the three parameters is
282 generally and occasionally observed in summer and later spring during our
283 experimental period. The characteristics of the diurnal variation of the RT height can
284 be represented better in Fig. 11, which shows the mean Lomb-Scargle power spectrum
285 of the RT as a function month during November 2011-May 2017. As compared with
286 other months, the dominant diurnal periodicity is less evident in April. We need to
287 clarify that atmospheric tides are of course not the only source of the diurnal variation

288 in tropopause height, diurnal convective activities (Yamamoto et al., 2003) might also
289 be an important cause. Here will not be **discussed in detail**.

290

291 **4. Discussion**

292 As for the radar echo power definition, the RT estimation sometimes will fail due
293 to the system problems, even if the thermal tropopause is well defined (Hall et al., 2009).
294 Apart from the system problems (**e.g. the damage of T/R module**), the following two
295 conditions are primarily responsible for the failure (or difficulty) of both the radar and
296 thermal definitions over the radar site latitude ($\sim 40^\circ$ N). Firstly, the temperature
297 sometimes continued to decrease **until to the stratosphere** (above 16 km) in summer and
298 early autumn, leading to the failure/difficulty of both the radar and thermal definitions
299 (a typical case as shown in Fig. 12a). Need to note that the temperature inversion layer
300 occurred at ~ 16 km in summer or early autumn is the second tropopause with
301 characteristics of Tropics (Pan et al., 2004; Randel et al., 2007). Secondly, some specific
302 meteorological processes can lead to the ambiguities and indefiniteness in thermal and
303 radar definitions, such as fronts, cyclones or typhoons, and folding (e.g. Nastrom et al.,
304 1989; May et al., 1991; Roettger, 2001; Alexander et al., 2013). Such ambiguities often
305 result in large difference in altitude between the RT and LRT. **In addition**, when multiple
306 temperature inversion layers occurred (below 16 km), the RT sometimes matched the
307 lower **layer with enhanced echo power** and LRT often matched the upper **layer** (e.g.
308 Yamamoto et al., 2003; Fukao et al., 2003). Apart from the situations above, **another**
309 **condition is also commonly** responsible for **the difficult in identifying the thermal**

310 tropopause from radiosonde profiles during summer. As a typical case shown in Fig.
311 12b, a significant inversion in temperature (at ~12 km) is recorded from the radiosonde
312 profile, but the altitude extent of inversion layer is too thin to meet the WMO criterion
313 that thermal definition required. Whereas, the apparent enhancement in radar echo
314 power corresponding to such inversion layer is strong enough to well define the RT.
315 The temperature inversion located near ~16 km (the second tropopause) is not the focus
316 of this paper.

317 Pan et al., (2004) have reported that the difference between the LRT and PVT are
318 more distinct in the vicinity of subtropical jet. In the northern hemisphere, the axis of
319 the subtropical jet is situated near ~30°N in spring and winter, whereas in summer and
320 early autumn the subtropical jet shifts northward to ~40°N (see Fig. 4 in Ding and Wang,
321 2006). We preliminary considered that the inconsistency between the RT and PVT in
322 summer and early autumn (Fig. 6c and 6d) is most likely related to the subtropical jet
323 shifting poleward to ~40°N. The existing cyclones or anticyclones in the upper-
324 troposphere (Wirth, 2000), of course, may also be an important influence factor for the
325 significant asymmetric differences (most of the scattered points deviate significantly
326 from the 1:1 line). The asymmetric differences, that is most of the RT are located higher
327 than the 2PVU tropopause height, suggest that the 2PVU surface is not the best measure
328 of a dynamical tropopause over Beijing during summer-time. More detailed discussion
329 about the striking asymmetric differences in height between LRT and PVT can be seen
330 in Wirth (2001) and will not be given here. Anyway, we need to be careful when using
331 the 2PVU dynamical definition to define the tropopause over radar site latitude ~40° N,

332 especially in summer.

333 About the characteristics of tropopause and the comparison between different
334 definitions, there are many differences between mid-latitude and polar regions. In mid-
335 latitude ($\sim 40^\circ\text{N}$), our results show that: (1) the agreement between RT and LRT is
336 similar good throughout the seasons; (2) RTs are generally located higher than the LRT;
337 (3) the thermal definition sometimes fail in summer and early autumn; (4) the
338 agreement between the RT/LRT and PVT in summer is poor. Whereas, in contrast,
339 previous researches about the tropopause over polar regions **reported** that (Wirth, 2000;
340 Alexander et al., 2013): (1) the difference between the RT and LRT is larger during
341 winter than that during summer; (2) RTs are generally located lower than the LRT; (3)
342 the thermal definition sometimes fail in winter and spring; (4) **the** comparison between
343 the RT and PVT showed the similar good agreement during both summer and winter.

344 Over a polar latitude station, the seasonal characteristics of the diurnal oscillation
345 in tropopause height were investigated using 5 years of SOUSY VHF radar
346 measurements (Hall, 2013b). The sunlight variability in polar regions is different from
347 that in other latitudes of the world. Different sunlight variation actually will lead to
348 difference in atmospheric tides, and then would result in different diurnal variation in
349 tropopause height. Here we found that the diurnal oscillation of RT height at Xianghe
350 is ubiquitous and obvious throughout the seasons except for April (Fig. 11). Whereas at
351 polar latitude and in months of November to February when there is no sunlight, Hall
352 (2013b) observed little evidence of 24 h diurnal variability in RT height.

353

354 5. Conclusions

355 In this paper, we present the high resolution structure and variability of the
356 tropopause in Xianghe, China (39.75° N, 116.96° E), based on the Beijing MST radar
357 vertical beam echo power data collected during the period November 2011-May 2017.
358 Fine-scale structure of the RT is well determined with a high temporal resolution of 0.5
359 h. Comparison results have shown good agreement in altitude between the RT and LRT,
360 with a correlation coefficient of ≥ 0.74 for the four seasons. Higher tropopause
361 sharpness seems to contribute lower difference between the RT and LRT in altitude and
362 weaker sharpness appears responsible for higher difference. The agreement between the
363 RT and PVT is relatively well in winter and spring with correlation coefficient of 0.72
364 and 0.76 respectively, but poor during summer with a correlation coefficient of only
365 0.33. We initially suggested that the poor consistency between RT and PVT is associated
366 with the subtropical jet shifting poleward to $\sim 40^\circ\text{N}$.

367 As expected, the sudden jump in static stability (represented by the buoyancy
368 frequency squared) and the rapid increase in radar echo power upon the tropopause
369 layer are clearly observed. Upon the tropopause layer, a sudden increase in effective
370 radar data acquisition rate is also observed. Both the monthly mean RT and LRT height
371 have shown a clear annual cycle. The variability and oscillation of RT height with
372 diurnal or lower timescales is presented. Obvious diurnal variation in tropopause height,
373 zonal wind, and meridional wind is generally observed throughout the seasons,
374 indicating the modulation most likely from the atmospheric tides. The semidiurnal
375 variation in RT height is not so obvious and commonly observed occasionally in

376 summer and late spring.

377

378 **Acknowledgment**

379 This work is funded by National Natural Science Foundation of China (NSFC grants
380 No. 41474132 and 41722404). We acknowledge the Chinese Meridian Project for
381 providing the MST radar data. The authors sincerely acknowledge the ECMWF for
382 providing global reanalysis data. The MST radar data for this paper are available at Data
383 Centre for Meridian Space Weather Monitoring Project (<http://159.226.22.74/>). The
384 radiosonde data are publicly available from the NOAA/ESRL Database at
385 <https://ruc.noaa.gov/raobs/>.

386

387 **References**

388 Alexander, S.P., Murphy, D.J., and Klekociuk, A.R.: High resolution VHF radar
389 measurements of tropopause structure and variability at Davis, Antarctica (69° S,
390 78° E), *Atmos. Chem. Phys.*, 13, 3121-3132, 2013.

391 Angell, J. K., and Korshover, J.: Quasi-biennial and long-term fluctuations in
392 tropopause pressure and temperature, and the relation to stratospheric water vapor
393 content. *Monthly Weather Review*, 102(1), 29-34, 2009.

394 Appenzeller, C., Holton, J. R., and Rosenlof, K. H.: Seasonal Variation of Mass
395 Transport Across the Tropopause. *Journal of Geophysical Research*, 101(D10),
396 15071-15078, 1996.

397 Añel, J. A., J. C. Antuña, L. de la Torre, R. Nieto, and Gimeno L.: Changes in tropopause

398 height for the Eurasian region determined from CARDS radiosonde data.
399 *Naturwissenschaften*, 93, 603–609, doi:10.1007/s00114-006-0147-5, 2006.

400 Bethan, S., Vaughan, G., and Reid, S. J.: A comparison of ozone and thermal tropopause
401 heights and the impact of tropopause definition on quantifying the ozone content
402 of the troposphere. *Quarterly Journal of the Royal Meteorological Society*,
403 122(532), 929-944, 1996.

404 Baray, J., Daniel, V., Ancellet, G., and Legras, B.: Planetary-scale tropopause folds in
405 the southern subtropics. *Geophysical Research Letters*, 27(3), 353-356, 2000.

406 Chen, F. L., Chen, G., Shi, C. H., Tian, Y. F., Zhang, S. D., and Huang, K. M.: Strong
407 downdrafts preceding rapid tropopause ascent and their potential to identify cross-
408 tropopause stratospheric intrusions, *Annales Geophysicae*, 36(5), 1403-1417,
409 2018.

410 Chen, G., Cui, X., Chen, F., Zhao, Z., Wang, Y., Yao, Q., and Gong, W.: MST Radars
411 of Chinese Meridian Project: System Description and Atmospheric Wind
412 Measurement. *IEEE Transactions on Geoscience and Remote Sensing*, 54(8),
413 4513-4523, 2016.

414 Das, S. S., Jain, A. R., Kumar, K. K., and Rao, D. N.: Diurnal variability of the tropical
415 tropopause: Significance of VHF radar measurements. *Radio Science*, 43(6), 1-14,
416 doi:10.1029/2008RS003824, 2008.

417 Dee, D. P., Uppala, S. M., Simmons, A. J., Berrisford, P., Poli, P., Kobayashi, S. et al.:
418 The ERA-Interim reanalysis: configuration and performance of the data
419 assimilation system. *Quarterly Journal of the Royal Meteorological Society*,

420 137(656), 553-597, 2011.

421 Ding, A., and Wang, T.: Influence of stratosphere-to-troposphere exchange on the
422 seasonal cycle of surface ozone at Mount Waliguan in western China. *Geophysical*
423 *Research Letters*, 33(3), 233-252, doi:10.1029/2005GL024760, 2006.

424 Fukao, S., H. Hashiguchi, M. Yamamoto, T. Tsuda, T. Nakamura, M. K. Yamamoto,
425 T. Sato, M. Hagio, and Y. Yabugaki.: Equatorial Atmosphere Radar (EAR):
426 System description and first results. *Radio Science*, 38(3), 1053, 2003.

427 Gage, K. S., and Green, J. L.: An objective method for the determination of tropopause
428 height from VHF radar observations. *Journal of Applied Meteorology*, 21(21),
429 1150-1154, 1982.

430 Gage, K. S., and Green, J. L.: Tropopause Detection by Partial Specular Reflection with
431 Very-High-Frequency Radar. *Science*, 203(4386), 1238-1240, 1979.

432 Gettelman, A., P. Hoor, L. L. Pan, W. J. Randel, M. I. Hegglin, and T. Birner: The
433 extratropical upper troposphere and lower stratosphere, *Reviews of Geophysics*,
434 49(3), RG3003, doi: 10.1029/2011RG000355, 2011.

435 Hermawan, E., Tsuda, T., and Adachi, T.: MU radar observations of tropopause
436 variations by using clear air echo characteristics. *Earth, Planets and Space*, 50(4),
437 361-370, 1998.

438 Hall, C.: The radar tropopause above Svalbard 2008–2012: Characteristics at various
439 timescales. *Journal of Geophysical Research*, 118(6), 2600-2608, 2013a.

440 Hall, C.: The radar tropopause at 78°N, 16°E: Characteristics of diurnal variation.
441 *Journal of Geophysical Research*, 118(12), 6354-6359, doi:10.1002/jgrd.50560,

442 2013b.

443 Hall, C. M., Röttger, J., Kuyeng, K., Sigernes, F., Claes, S., and Chau, J. L.: Tropopause
444 altitude detection at 78°N, 16°E, 2008: First results of the refurbished SOUSY
445 radar. *Radio Science*, 44(5), 1-12, doi:10.1029/2009RS004144, 2009.

446 Hoinka, K. P.: Statistics of the Global Tropopause Pressure. *Monthly Weather Review*,
447 126(12), 3303-3325, 1998.

448 Hoskins, B. J., McIntyre, M. E., and Robertson, A. W.: On the use and significance of
449 isentropic potential vorticity maps. *Quarterly Journal of the Royal Meteorological*
450 *Society*, 111(470), 877-946, 2007.

451 Huang, C., Zhang, S. D., Zhou, Q. H., Yi, F., Huang, K., Gong, Y., Zhang, Y., and Gan,
452 Q.: WHU VHF radar observations of the diurnal tide and its variability in the lower
453 atmosphere over Chongyang (114.14° E, 29.53° N), China. *Annales Geophysicae*,
454 33(7), 865-874, 2015.

455 Hoerling, M. P., Schaack, T. K., and Lenzen, A. J.: Global Objective Tropopause
456 Analysis. *Monthly Weather Review*, 119(8), 1816-1831, 1991.

457 Liu, Y., Xu, T., and Liu, J.: Characteristics of the seasonal variation of the global
458 tropopause revealed by cosmic/GPS data. *Advances in Space Research*, 54(11),
459 2274-2285, 2014.

460 May, P. T., Yamamoto, M., Fukao, S., Sato, T., Kato, S., and Tsuda, T.: Wind and
461 reflectivity fields around fronts observed with a VHF radar. *Radio Science*, 26(5),
462 1245-1249, 1991.

463 Nastrom, G. D., Green, J. L., Gage, K. S., and Peterson, M. R.: Tropopause Folding and
464 the Variability of the Tropopause Height as Seen by the Flatland VHF Radar.
465 *Journal of Applied Meteorology*, 28(12), 1271-1281, 1989.

466 Nielsen-Gammon, J. W.: A visualization of the global dynamic tropopause. *Bulletin of*
467 *the American Meteorological Society*, 82(6), 1151-1168, 2001.

468 Pan, L. L., Randel, W. J., Gary, B. L., Mahoney, M. J., and Hints, E. J.: Definitions
469 and sharpness of the extratropical tropopause: A trace gas perspective. *Journal of*
470 *Geophysical Research*, 109, D23103, doi:10.1029/2004JD004982, 2004.

471 Pan, L. L., W. J. Randel, J. C. Gille, W. D. Hall, B. Nardi, S. Massie, V. Yudin, R.
472 Khosravi, P. Konopka, and D. Tarasick: Tropospheric intrusions associated with
473 the secondary tropopause, *Journal of Geophysical Research*, 114, D10302, 2009.

474 Press, W. H., and Rybicki, G. B.: Fast algorithm for spectral analysis of unevenly
475 sampled data. *The Astrophysical Journal*, 338(1), 277-280, 1989.

476 Ravindrababu, S., Venkat Ratnam, M., Sunilkumar, S. V., Parameswaran, K., and
477 Krishna Murthy, B. V.: Detection of tropopause altitude using Indian MST radar
478 data and comparison with simultaneous radiosonde observations. *Journal of*
479 *Atmospheric and Solar-Terrestrial Physics*, 121(6), 679-687, 2014.

480 Randel, W. J., Wu, F., and Gaffen, D. J.: Interannual variability of the tropical
481 tropopause derived from radiosonde data and NCEP reanalyses. *Journal of*
482 *Geophysical Research Atmospheres*, 105(D12), 15509-15523, 2000.

483 Randel, W. J., Seidel, D. J., and Pan, L. L.: Observational characteristics of double
484 tropopauses. *Journal of Geophysical Research*, 112, D07309, 2007.

485 Randel, W. J., and Wu, F.: The Polar Summer Tropopause Inversion Layer. *Journal of*
486 *the Atmospheric Sciences*, 67(8), 2572-2581, 2010.

487 Randel, W. J., Wu, F., and Forster, P. M.: The extratropical tropopause inversion layer:
488 Global observations with GPS data, and a radiative forcing mechanism. *Journal of*
489 *the Atmospheric Sciences*, 64(12), 4489-4496, 2007.

490 Ramakrishnan, K. P.: Distortion of the tropopause due to meridional movements in the
491 sub-stratosphere. *Nature*, 132(3346), 932-932, 1933.

492 Roettger, J.: Observations of the polar d-region and the mesosphere with the Eiscat
493 Svalbard radar and the SOUSY Svalbard Radar (scientific paper). *Memoirs of*
494 *National Institute of Polar Research. Special Issue*, 54(94), 9-20, 2001.

495 Reed, R. J.: A study of a characteristic type of upper-level frontogenesis. *Journal of the*
496 *Atmospheric Sciences*, 12(3), 226-237, 1955.

497 Santer, B. D., Wehner, M. F., Wigley, T. M., Sausen, R., Meehl, G. A., Taylor, K. E.,
498 Ammann, C., Arblaster, J., Washington, W. M., Boyle, J. S., and Brüggemann, W.:
499 Contributions of anthropogenic and natural forcing to recent tropopause height
500 changes. *Science*, 301(5632), 479-483, 2003.

501 Santer, B. D., Sausen, R., Wigley, T. M., Boyle, J. S., Achutarao, K., Doutriaux, C.,
502 Hansen, J. E., Meehl, G. A., Roeckner, E., Ruedy, R., Schmidt, G., and Taylor, K.
503 E.: Behavior of tropopause height and atmospheric temperature in models,
504 reanalyses, and observations: Decadal changes. *Journal of Geophysical Research*,
505 108(D1), 4002, doi:10.1029/2002JD002258, 2003a.

506 Sausen, R., and Santer, B. D.: Use of Changes in Tropopause Height to Detect Human

507 Influences on Climate. *Meteorologische Zeitschrift*, 12(3), 131-136, 2003.

508 Schmidt, T., Heise, S., Wickert, J., Beyerle, G., & Reigber, C.: GPS radio occultation
509 with CHAMP and SAC-C: global monitoring of thermal tropopause parameters.
510 *Atmospheric Chemistry and Physics*, 5(6), 1473-1488, 2005.

511 Seidel, D. J., Ross, R. J., Angell, J. K., and Reid, G. C.: Climatological characteristics
512 of the tropical tropopause as revealed by radiosondes. *Journal of Geophysical*
513 *Research*, 106(D8), 7857-7878, 2001.

514 Son, S. W., Tandon, N. F., & Polvani, L. M.: The fine-scale structure of the global
515 tropopause derived from COSMIC GPS radio occultation measurements. *Journal*
516 *of Geophysical Research: Atmospheres*, 116(D20), 2011.

517 Sprenger, M., Croci Maspoli, M., and Wernli, H.: Tropopause folds and cross-
518 tropopause exchange: a global investigation based upon ECMWF analyses for the
519 time period March 2000 to February 2001. *Journal of Geophysical Research*
520 *Atmospheres*, 108(12), 291-302, 2003.

521 Tian, Y., and Lu, D.: Comparison of Beijing MST Radar and Radiosonde Horizontal
522 Wind Measurements. *Advances in Atmospheric Sciences*, 34(1), 39-53. doi:
523 10.1007 / s00376-016-6129-4, 2017.

524 Vaughan, G., Howells, A., and Price, J. D.: Use of MST radars to probe the mesoscale
525 structure of the tropopause. *Tellus A*, 47(5), 759-765, 1995.

526 Wang, C.: Development of the Chinese meridian project. *Chinese Journal of Space*
527 *Science*, 30(4), 382–384, 2010.

528 Wilcox L.J., Hoskins B.J., Shine K.P. 2012. A global blended tropopause based on ERA

529 data. Part I: Climatology. Q. J. R. Meteorol. Soc. 138: 561–575.

530 DOI:10.1002/qj.951.

531 Wirth, V.: Thermal versus dynamical tropopause in upper-tropospheric balanced flow
532 anomalies. Quarterly Journal of the Royal Meteorological Society, 126(562), 299-
533 317, 2000.

534 Wirth, V.: Cyclone-anticyclone asymmetry concerning the height of the thermal and the
535 dynamical tropopause. Journal of the Atmospheric Sciences, 58(1), 26-37, 2001.

536 WMO: Definition of the tropopause. WMO Bull., 6, 136, 1957.

537 Yamamoto, M., Oyamatsu, M., Horinouchi, T., Hashiguchi, H., and Fukao, S.: High
538 time resolution determination of the tropical tropopause by the Equatorial
539 Atmosphere Radar. Geophysical Research Letters, 30(21), 2094, 2003.

540 Zängl, G., and Hoinka, K. P.: The tropopause in the polar regions. Journal of Climate,
541 14(2001), 3117-3139, 2001.

542

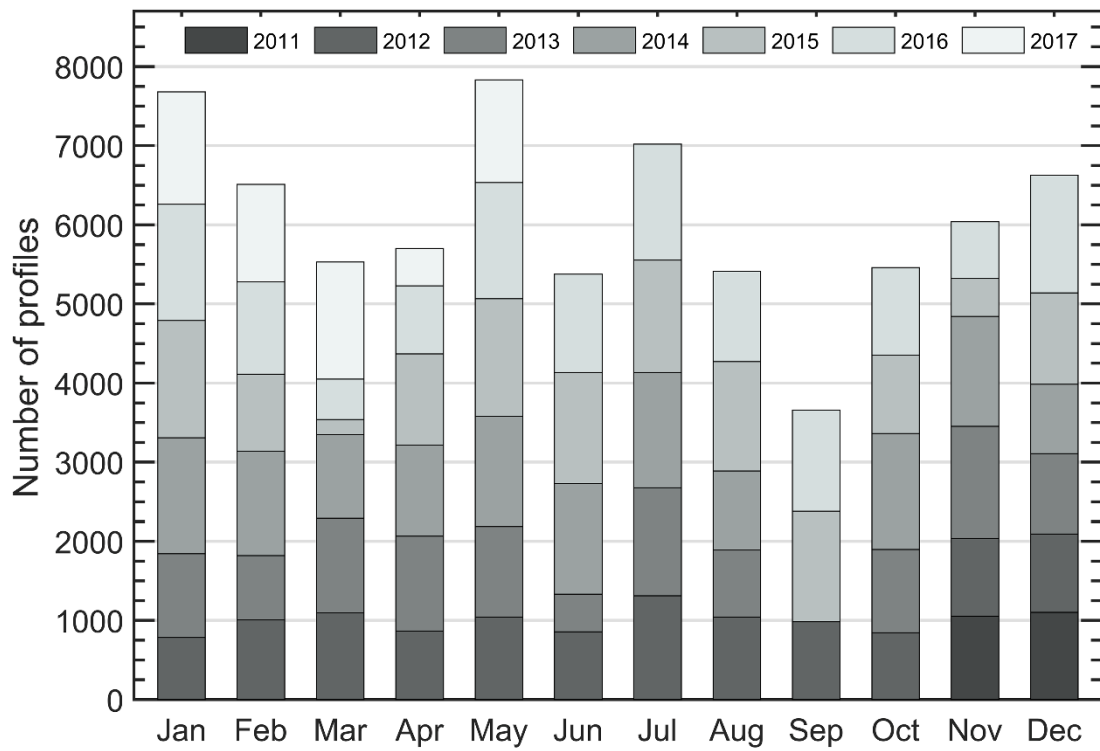
543 **Table**

Radar parameter	Value
Transmitted frequency	50 MHz
Antenna array	24×24 3-element Yagi
Antenna gain	33 dB
Transmitter peak power	172 kW
Code	16-bit complementary
No. coherent integrations	128 (low mode)/64 (mid mode)
No. FFT points	256
No. spectral average	10
Pulse repetition period	160 (low mode)/320 (mid mode) μ s
Half power beam width	3.2°
Pulse length	1 (low mode)/4 (mid mode) μ s
Range resolution	150 (low mode)/600 (mid mode) m
Temporal resolution	30 min
Off-zenith angle	15°

544 **Table 1.** Routine operational parameters in low and middle mode for the Beijing MST

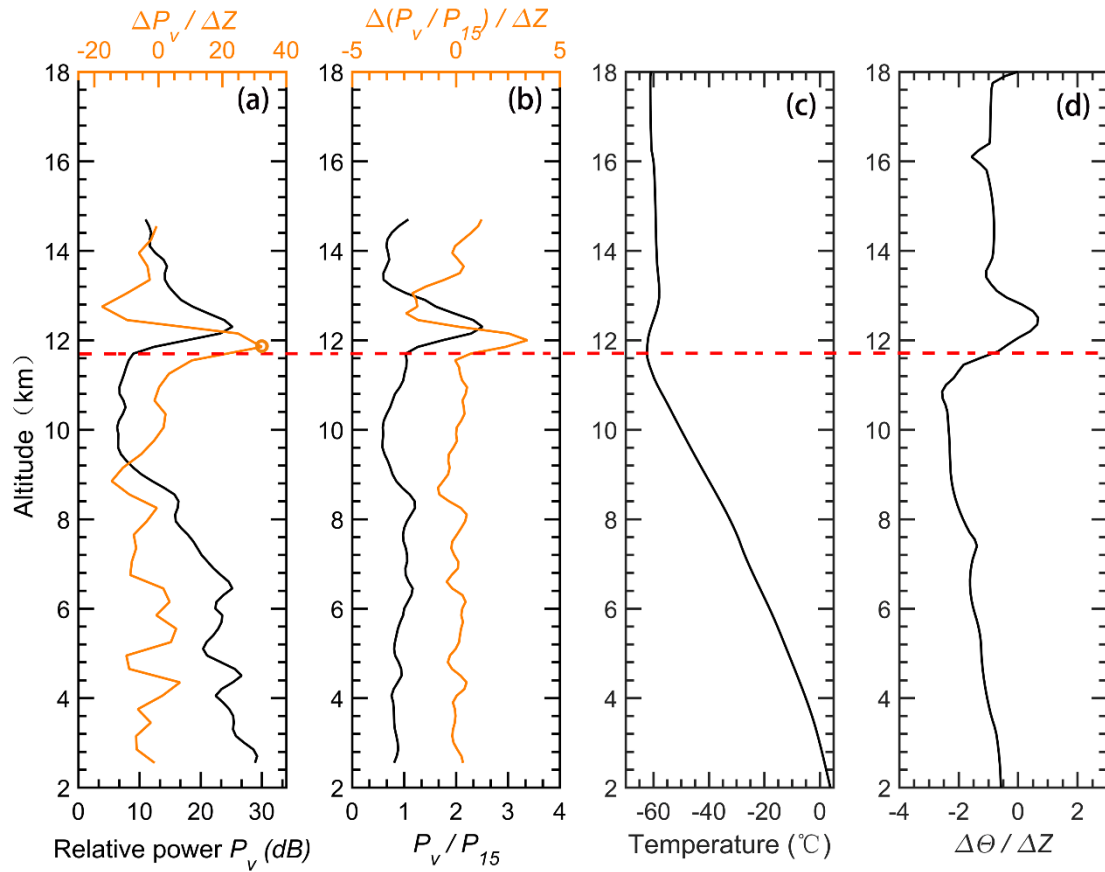
545 radar used in this study.

546



548

549 **Figure 1.** Distribution of the monthly total number of radar return echo power profiles
 550 that available from vertical beam in low mode, collected for the period November 2011-
 551 May 2017.



552

553 **Figure 2.** Example vertical profiles of (a) relative radar echo power (black line) along

554 with its gradient variation (orange line), (b) radar aspect sensitivity (black line) along

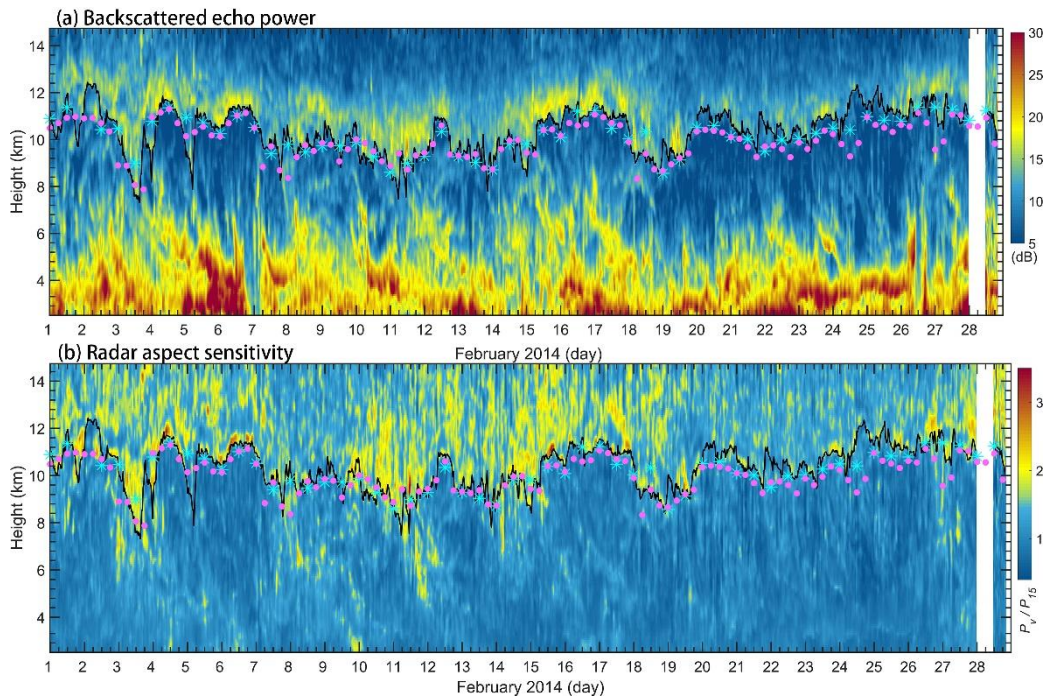
555 with its gradient variation (orange line), (c) radiosonde temperature and (d) potential

556 temperature gradient on 00 UT 04 November 2011. The horizontal red dashed line

557 marks the LRT height. The orange circle in Fig. 2a denotes the RT height.

558

559



560

561 **Figure 3.** Altitude-time intensity plot of (a) radar backscattered echo power and (b)

562 radar aspect sensitivity for February 2014. The tropopauses determined based on the

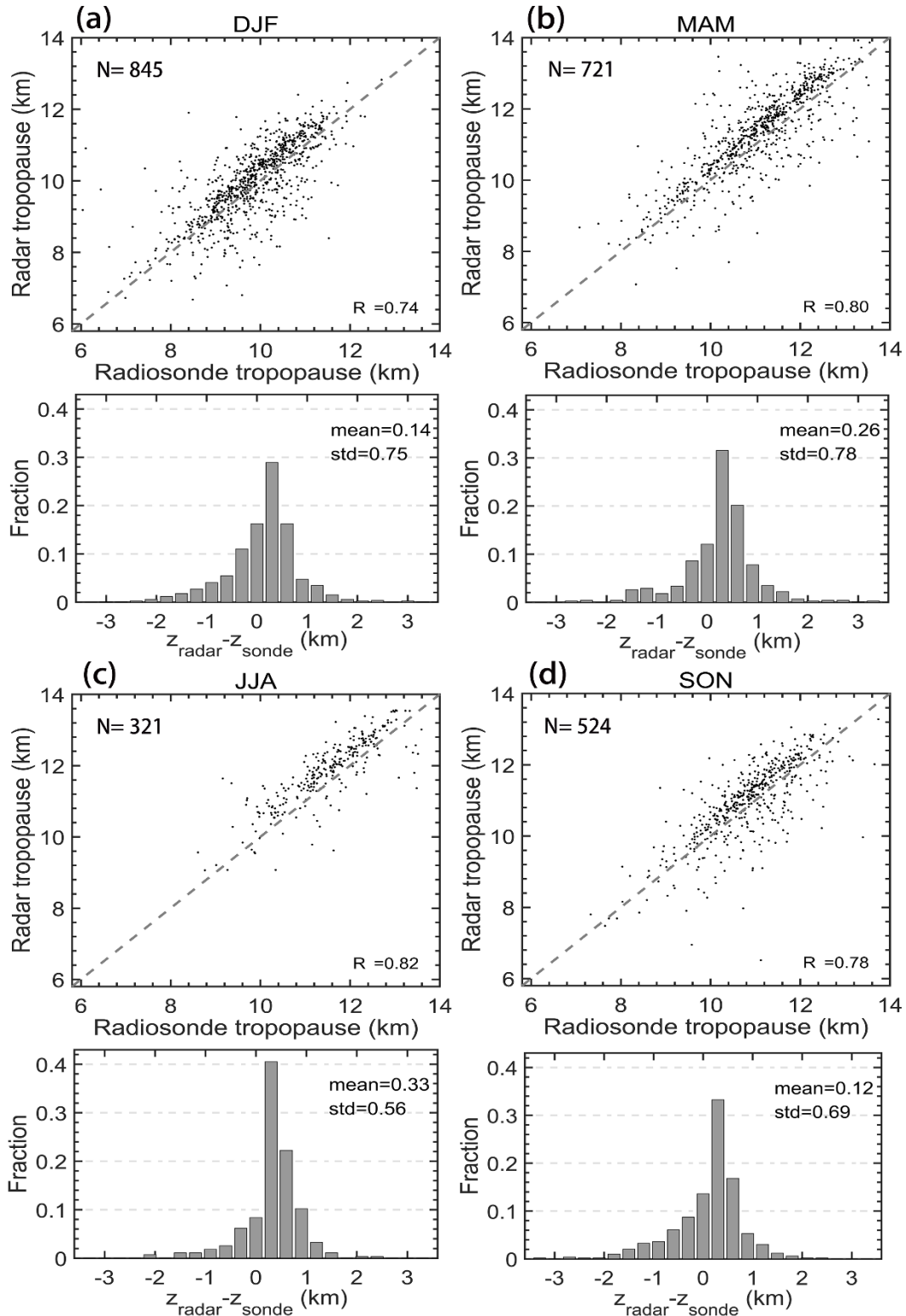
563 radar echo definition are shown as a black solid curve. The cyan asterisks ‘*’ and pink

564 dots indicate the location of the LRT derived from simultaneous twice daily radiosonde

565 data and the PVT from ECMWF ERA-Interim reanalysis, respectively. White stripe

566 indicates the time frame of radar missing data.

567



568

569 **Figure 4.** Seasonal scatterplots of the RT versus LRT and histogram distribution of

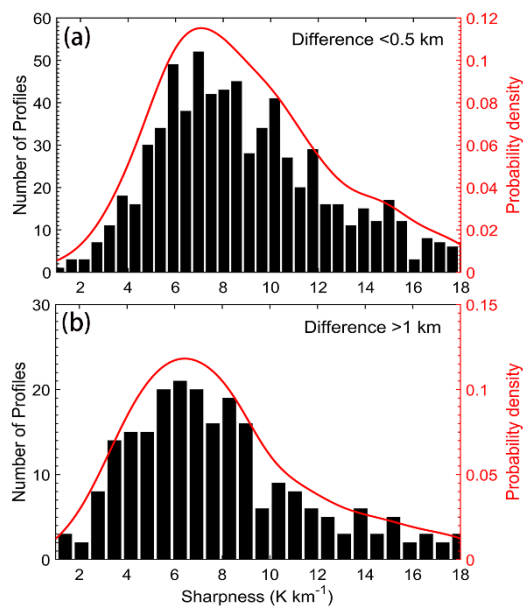
570 altitude differences between the RT and the LRT, for (a) winter DJF, (b) spring MAM,

571 (c) summer JJA, and (d) autumn SON, during the period November 2011-May 2017.

572 The positive values in the histogram indicate the RT locating at a higher level than the
573 LRT. The grey dashed line shows the 1:1 line. Here, 'N', 'R²', 'mean', and 'std' indicate
574 the sample numbers, correlation coefficient, mean difference, and standard deviation of
575 the difference, respectively.

576

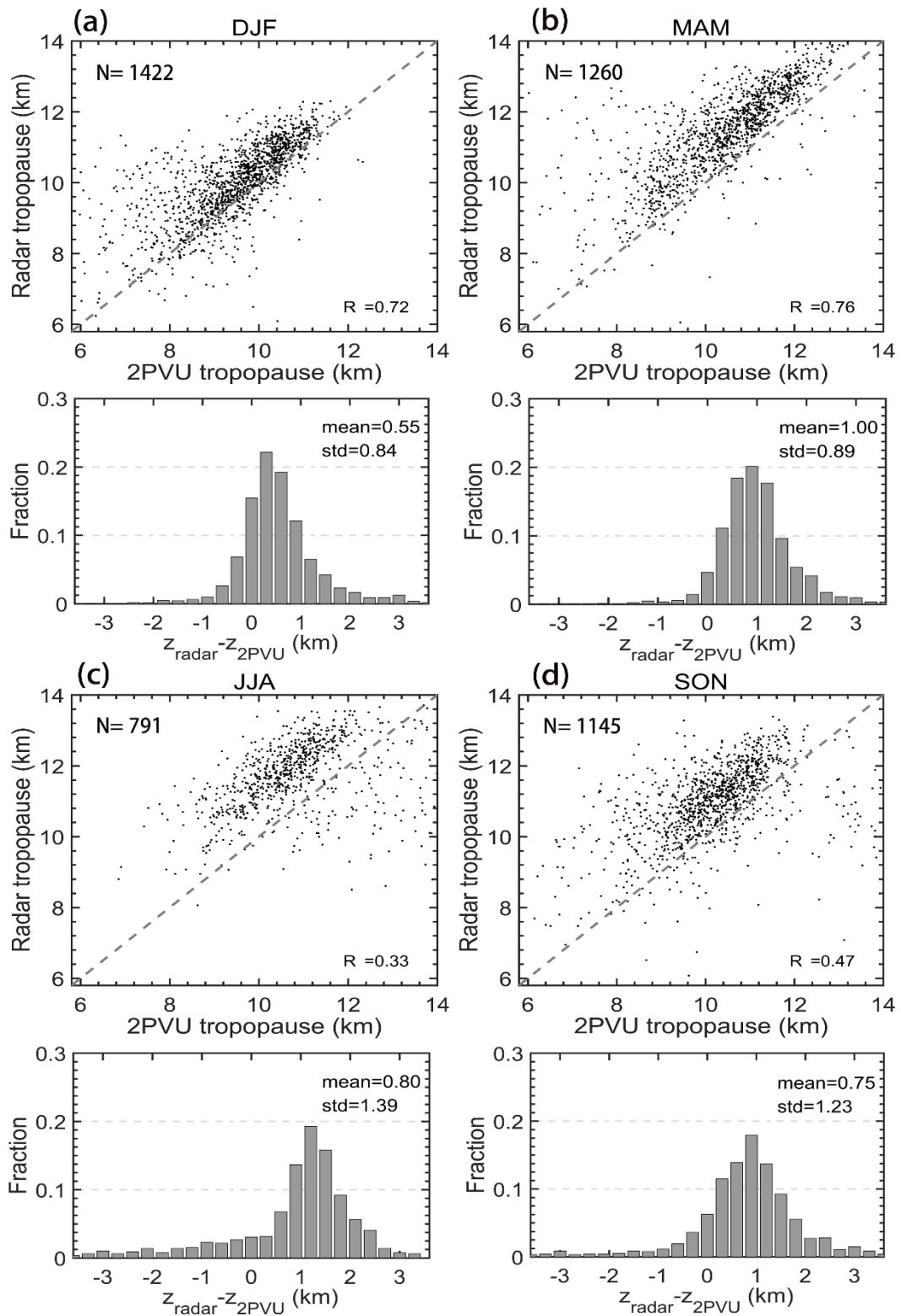
577



578

579 **Figure 5.** Histogram distribution of the tropopause sharpness for (a) difference < 0.5 km,
580 and (b) > 1 km respectively between the LRT and the RT.

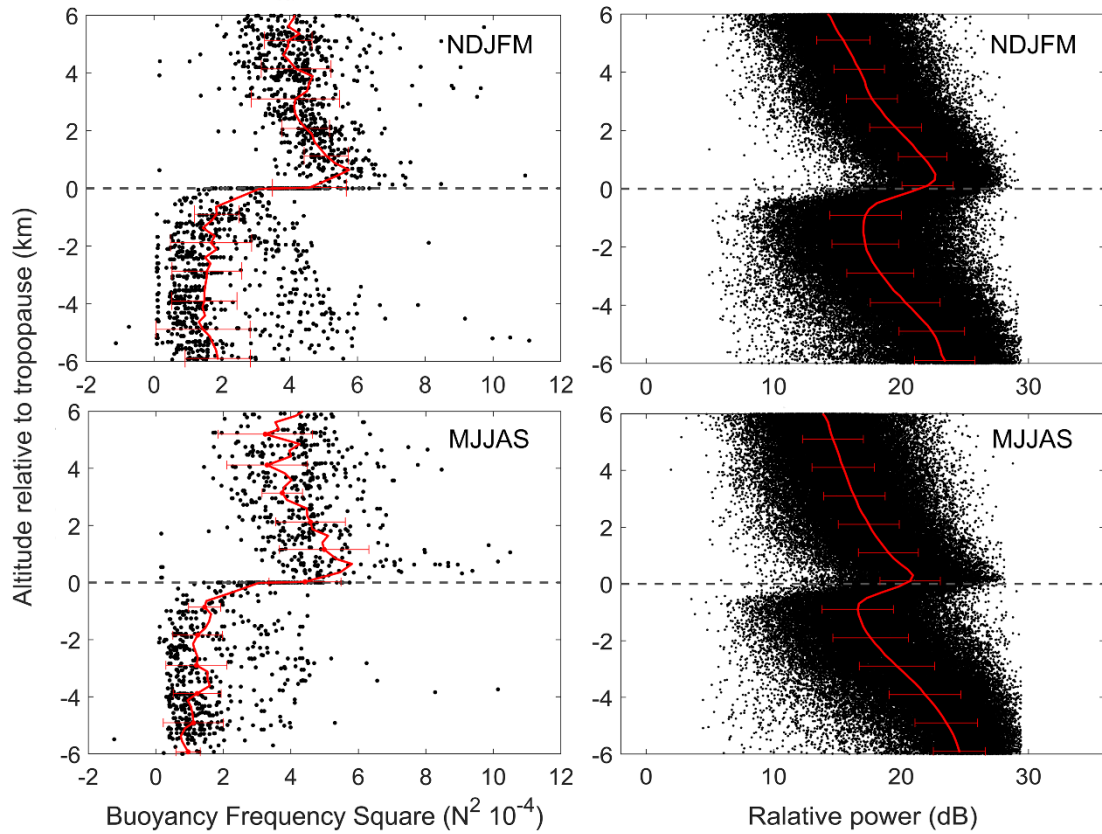
581



582

583 **Figure 6.** Same as figure 4, but for the comparison between the RT and the PVT.

584

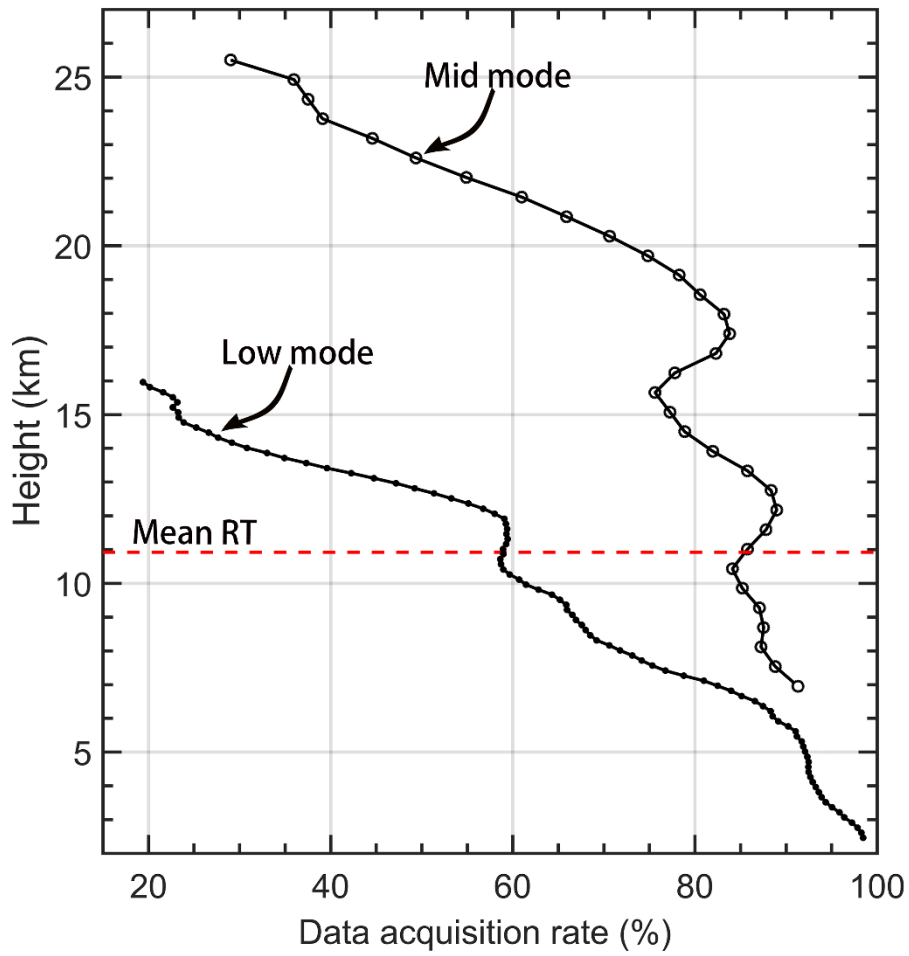


585

586 **Figure 7.** Scatterplots of (left panels) static stability (N^2) and (right panels) radar
 587 relative echo power as a function of altitude relative to the LRT (left panels) and RT
 588 (right panels) for extended winter (NDJFM) and summer (MJJAS) seasons for two
 589 specific years 2012-2013. Red lines in each panel denote the corresponding mean
 590 profiles and the error bars indicate the standard deviations.

591

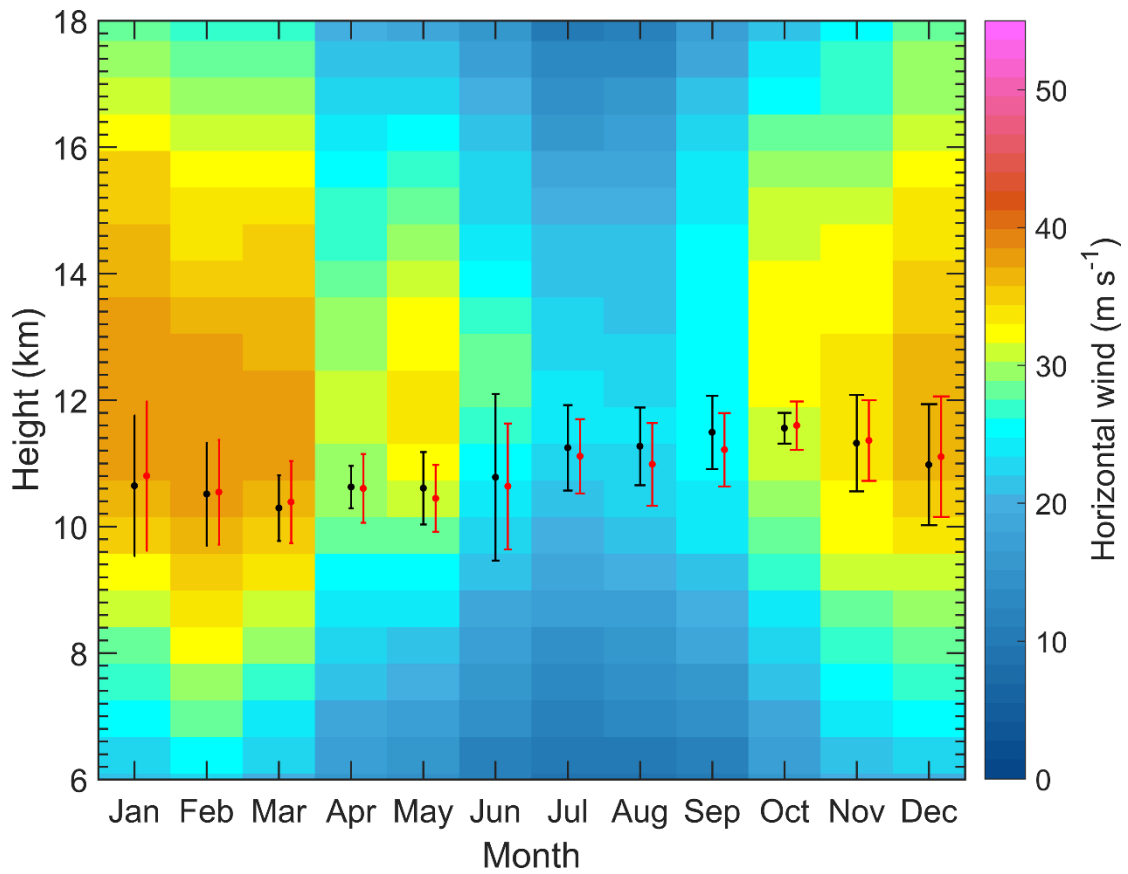
592



593

594 **Figure 8.** Vertical height profiles of the averaged effective radar **wind** data acquisition
 595 rate in low mode and middle mode during November 2011-May 2017. The red dashed
 596 line indicates the mean RT height.

597



598

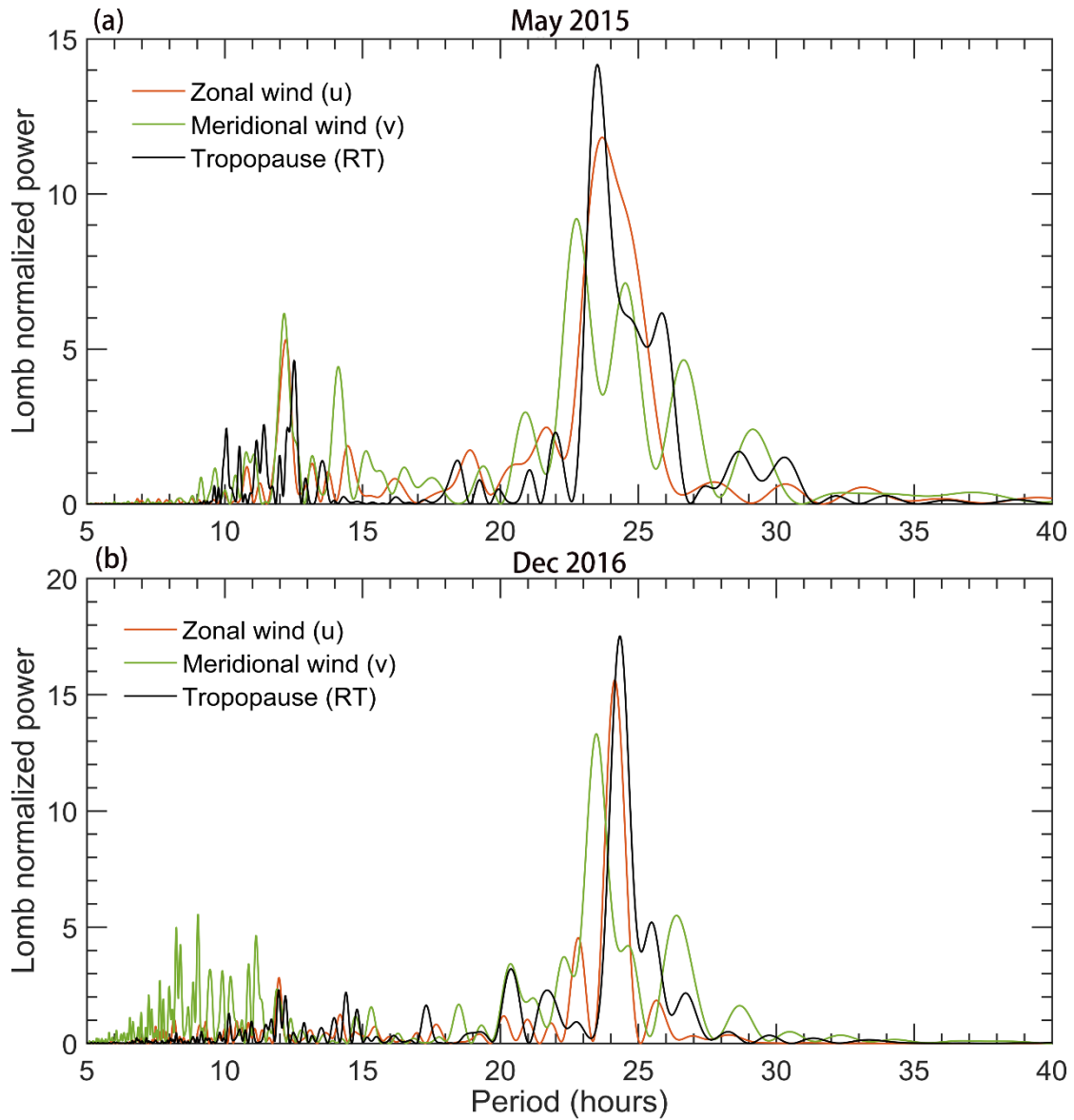
599 **Figure 9.** Height-time intensity map of monthly mean horizontal wind speed (shaded,

600 m/s) derived from the middle mode of Beijing MST radar, during November 2011-May

601 2017. Also shown is the monthly mean height of RT (black dots) and LRT (red dots,

602 offset by +6 days) along with the vertical error bars representing the standard deviations.

603



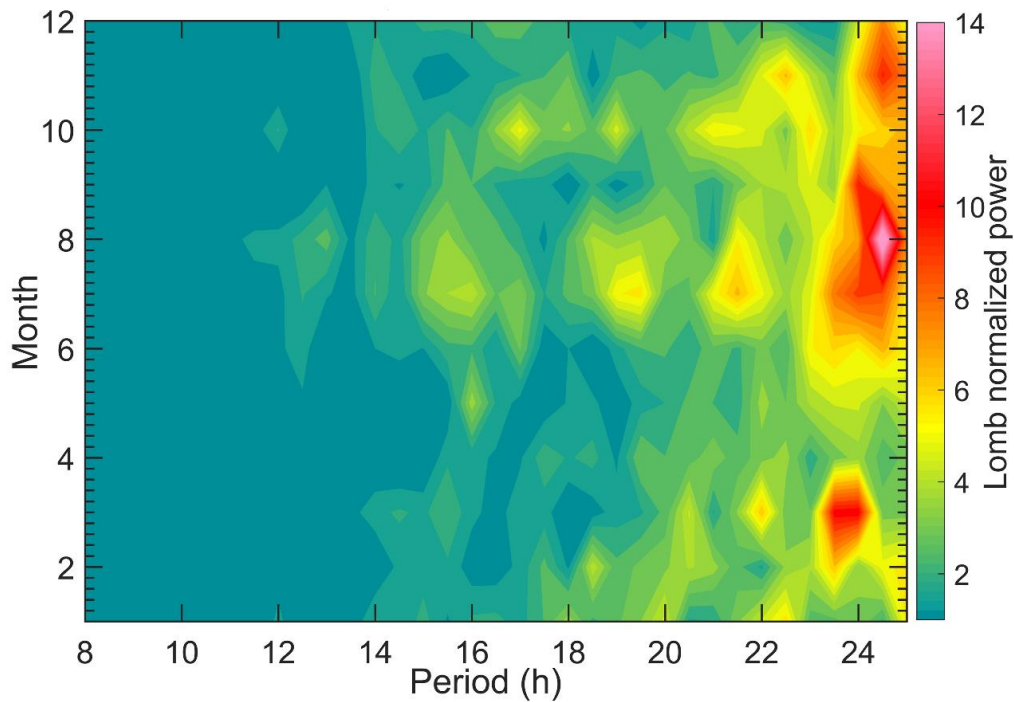
604

605 **Figure 10.** Lomb-Scargle periodograms of the RT height, zonal, and meridional wind

606 oscillations for specific months of (a) May 2015 and (b) December 2016. The zonal and

607 meridional wind for (a) is sampled at 9.85 km and (b) at 11 km.

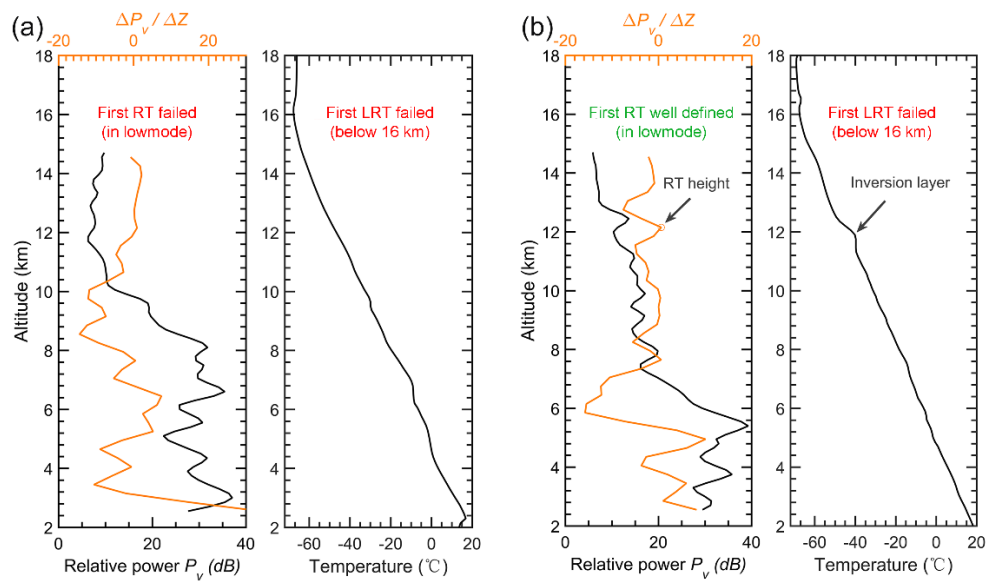
608



609

610 **Figure 11.** Mean Lomb-Scargle periodograms of RT height as a function of the time of

611 month during November 2011-May 2017.



612

613 **Figure 12.** Example profiles of radar echo power and radiosonde temperature that (a)

614 both the RT and LRT definitions fail due to the continuing decrease in temperature on

615 00 UTC 7 July 2012 and (b) the temperature inversion layer failed to meet the LRT

616 definition but well defined in RT definition on 12 UTC 02 August 2012. **Please note**

617 **that we only consider the conditions below 16 km.**

